Deliverable 6.1

Summary report: Description of the thermal processes used for the thermal treatment of the RSOW and the physical properties and chemical composition of the resulting treated wastes

Date 30.8.2023 Version Final

Dissemination level Public

Hélène NONNET
CEA
BP17171
30207 Marcoule France

Helene.nonnet@cea.fr
+33 4 66 79 16 75

This project has received funding from the Euratom research and training programme 2019-2020 under grant agreement No 945098.

Project acronym PREDIS	**Project title** PRE-DISposal management of radioactive waste		**Grant agreement No.** 945098
Deliverable No. D6.1	**Deliverable title** Summary report: Description of the thermal processes used for the thermal treatment of the RSOW and the physical properties and chemical composition of the resulting treated wastes		**Version** Final
Type Report	**Dissemination level** Public		**Due date** M36
Lead beneficiary CEA			**WP No.** 6
Main author Hélène NONNET, CEA	**Reviewed by** Thierry MENNECART, WP6 leader, SCK CEN	**Accepted by** Maria Oksa, coordinator, VTT	
Contributing authors E. Torres, A. Bahillo (CIEMAT); E. Mossini, F. Galluccio, A. Santi, E. Rizzi, G. Magugliani, E. Macerata, M. Giola, M. Mariani (POLIMI) ; Yu. Zabulonov, B. Zlobenko, A. Pugach, A. Rozko, Yu. Fedorenko (SIIEG); Veli-Matti Pulkkanen (VTT); Hélène Nonnet (CEA); Josh Radford (USFD), Claire Corkhill (USFD); Vojtěch Galek (CVRez), Anna Sears (CVRez), Petr Pražák (CVRez), Martin Vacek (CVRez), Jak Hadrava (CVRez)			**Pages** 54

Abstract

This report presents descriptions of the different radioactive organic solids' treatment processes used and developed at CIEMAT, POLIMI, SIIEG, VTT, CEA, UFSD and CVRez.
It also describes the physico-chemical characteristics of the materials after these treatments.

Coordinator contact
Maria Oksa
VTT Technical Research Centre of Finland Ltd
Kivimiehentie 3, Espoo / P.O. Box 1000, 02044 VTT, Finland
E-mail: maria.oksa.@vtt.fi
Tel: +358 50 5365 844

Notification

Acknowledgement

This project has received funding from the Euratom research and training programme 2019-2020 under grant agreement No 945098.

TABLE OF CONTENTS

1 Thermal treatment of SIERs surrogates in CIEMAT

Contributing authors
E. Torres, A. Bahillo, CIEMAT

In Spain, thermal treatment, in particular, incineration is used for the management of liquid organic wastes, mostly scintillation cocktails. Scintillation cocktails (from non-nuclear producers) are incinerated at El Cabril disposal site and subsequently, ashes are solidified in mortar to solidify them in monolithic blocks. The incinerator used in the disposal facility is of the excess air type, with a double combustion chamber. A temperature of 800°C is reached in the first reactor, and 1000°C in the post-combustion chamber. At the chamber outlet there is a silicon carbide high-temperature filter. The fumes are cooled by dilution in fresh air to 140°C. The flue gases then pass through very high efficiency filters and once filtered are discharged through the stack.

Currently, experiments are ongoing abroad to treat decontamination effluents by incineration (slags and fly ashes will be sent back to Spain). Regarding Spent Ion Exchange Resins (SIERs), slurries from different purification systems are radiologically characterized and later, immobilized by cementation. After the radiological characterization of the waste packages, if they meet the WAC for disposal, they are shipped to the storage facility.

1.1 Preparation and characterization of surrogates

For PREDIS project, two types of IERs of frequent use in Spanish NPPs were chosen: a strong acid cationic type (Amberlite™ IRN-77) and a strong base anion type (Amberlite™ IRN-78). Both resins have a scaffold based on copolymers of styrene and divinylbenzene, being its characteristic functional groups sulphogroup –SO_3H (H-form of a resin) for cationic IRN77 and quaternary aminogroups anionic IRN-77.

Prior to the preparation of the surrogates, different waste streams from the primary and secondary circuits were examined, considering both chemical and radiological aspects. Doping of the SIERs surrogates was tailored assuming a target Volume Reduction Factor (VRF) of 5 so that, the activity of the final manufactured waste package could meet the WAC of the disposal facility.

Surrogates used for thermal treatment consisted of a mixed form of 50/50 cationic and anionic IERs, doped according to the specifications provided by two of our endusers. Resins were saturated with boron and traces of Sr, Cs and activation products (Co, Cr, Zn, Fe, Ag, Ni). For the saturation of the resins, doping solution was buffered to pH 10.2.

Before carrying out the thermal treatment of any material, a previous chemical analysis of the material is needed. In this case, a detailed chemical analysis of raw IRN77 and IRN78 and the doped mixture of IRN77/IRN78 (50:50) was carried out. Results are shown in Table 1 and Table 2.

Table 1. Elemental analysis (C, N, H, S) of raw IRN77 and IRN78 and the doped IRN77/IRN78 mix.

	IRN77	IRN78	Mix of doped IRN77 and IRN 78
Moisture, %	46,8	53,5	59±3
Carbon, %	27,4	32,3	49.0±0.1
Hydrogen, %	8,7	11,0	7.1±0.1
Sulfur, %	8,7	< 0,1	6.81±0.04
Nitrogen, %	< 0,1	2,7	2.22±0.03
Ash, %	< 0,1	< 0,1	< 0,1
C/H	3,1	2,9	6,9

Table 2. Chemical analysis of the doped mixture IRN77/IRN78 by a microwave digestion method (7:1 HNO_3 65%: H_2O_2 30%, temperature 190ºC).

Element	Doped IRN77/IRN78 mix
B	5%wt.
Element	***mg element/Kg doped IERs***
Ca	4,1
Co	5
Cr	5
Cs	30
Cu	2
Fe	10
Mg	1
Si	13
Sr	4,5
Zn	12

1.2 TGA analysis of the SIERs surrogates

Thermogravimetric analysis (TGA) is a technique that allows studying the behavior of materials in relation to temperature and their degradation over time. For this reason, the behavior in TGA of the doped resin will be compared before and after thermal treatment.

Figure 1 shows the behavior of IRN77 and IRN78 resins in TGA with nitrogen (IRN77N, IRN78N) and air (IRN77A, IRN78A). The results have been normalized to be able to compare them. Without attempting to enter into a deep discussion, three clearly differentiated phases are observed. The first stage corresponds up to 200ºC, to the loss of humidity, resin dehydration. IRN77 loses about 45%

in mass and IRN78 over 60% in mass. Reducing this moisture content is important so as not to excessively penalize the thermal efficiency of the reactor. Some of this moisture is lost when the resins are pre-dried at room temperature.

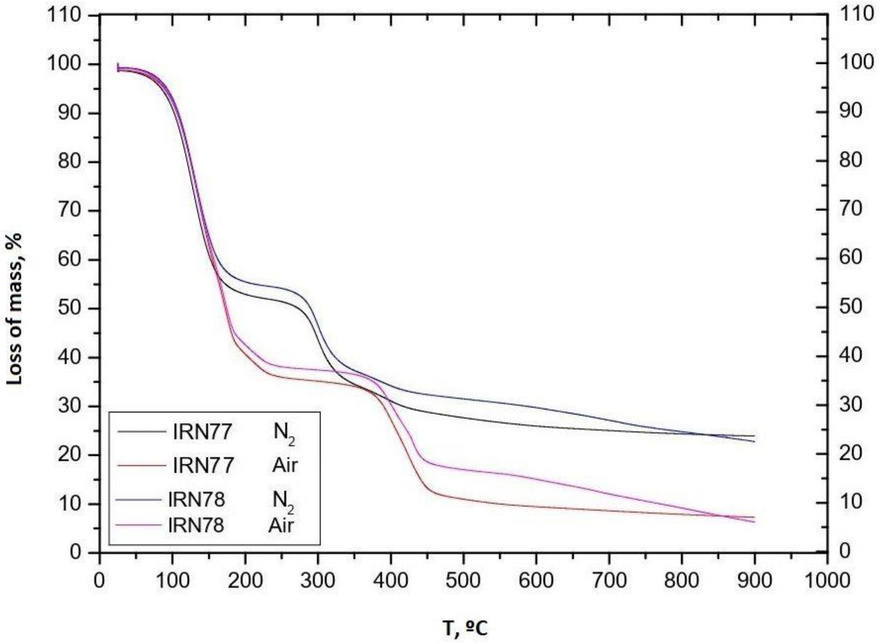

Figure 1. Evolution of loss of mass with the temperature of the resins without thermal treatment.

The mass loss in the second phase, in the temperature range of 200 – 450ºC corresponds to the loss of the volatile matter content of resins, about 25 – 30%. The difference between the tests carried out with air and nitrogen indicates the char content of the resins, about 20%.

Figure 2 shows the behavior of thermally treated doped IERs in TGA with nitrogen (IRN77N, IRN78N) and air (IRN77A, IRN78A). It is observed that there is no weight loss below 200 ºC, so there is no dehydration of the resins as expected. The ash content of the thermally treated resins is practically nil, similar to the original resins. Logically, the resins have been treated in the range of 450ºC, as they do not lose mass below that temperature. Higher temperatures are necessary to lose mass. The mass loss when N_2 is used as the fluid is representative of the volatile matter content. It is observed that in the treated resins some volatile matter remains, but what essentially remains is char.

Therefore, cationic and anionic resins with a high degree of humidity have been transformed into char, suitable for subsequent treatments. In addition, there is a significant mass loss, obtaining between 15 – 20% by mass of the initial resin and an equivalent volume reduction of 80% (VRF~5).

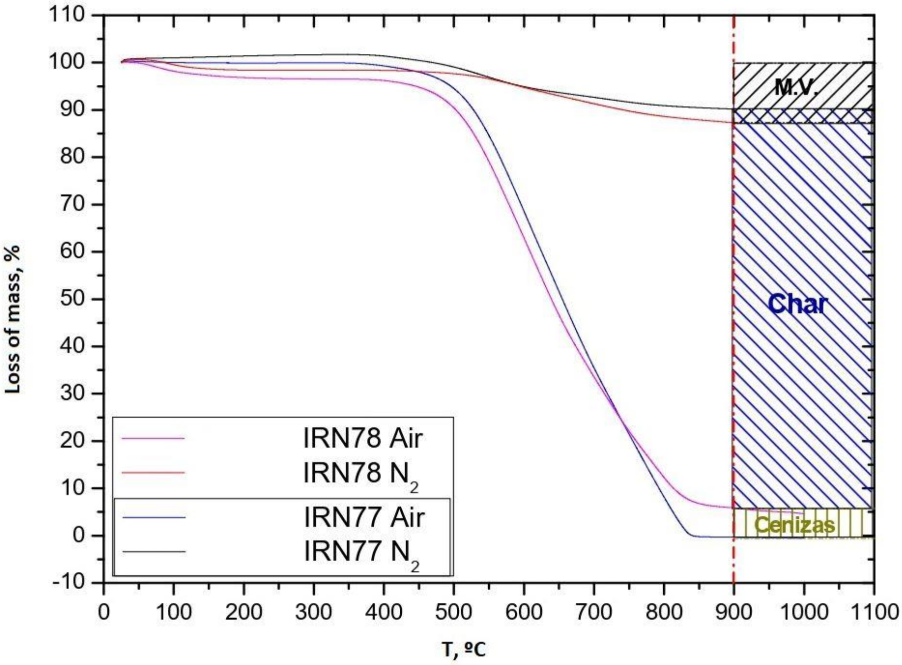

Figure 2. Evolution of mass loss with temperature of the resins during thermal treatment.

1.3 Lab-scale drop tube reactor

Experiments were developed in a laboratory-scale drop tube reactor, located at CIEMAT (Figure 3). The layout of the lab-combustor consists on a vertical quartz reactor tube of 1250 mm length and 50 mm internal diameter, built-in a 3 zone electric furnace, in which reacting solid particles are suspended in an upward flow of hot reactant gas. The lower zone of the furnace is used to pre-heat the reactant gas, which is introduced in the reactor through the lower section of the reactor tube, while the upper zone avoids heat losses, to keep isothermal conditions. The gas mixture selected for each experiment is set and fed by a mass- flow controller, being introduced through the base of the quartz tube. The out-coming gases are released through a side-arm at the top end of the tube, being conducted to a particulate control system, prior to gas analysis (Figure 4).

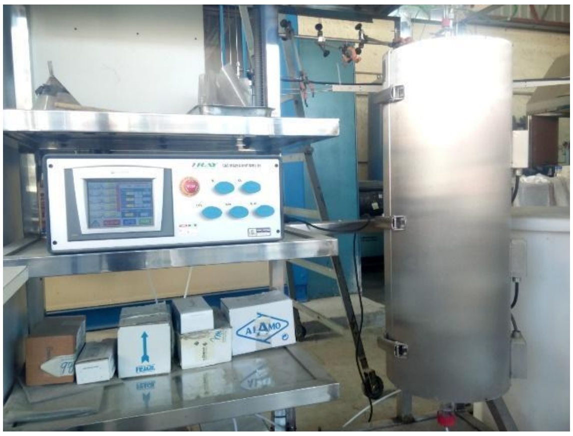

Figure 3. Laboratory-scale drop tube reactor in CIEMAT.

Three resins have been tested: doped IRN-77 (sulfonated cationic), doped IRN-78 (anionic) and a 50/50 mix of both resins. In order to reduce the moisture content of the resins, a pre-dehydration step, where the IERs slurries were exposed to room temperature. They lost about 35 – 40% of their initial weight. They were fed into the reactor by a screw feeder system, being combusted in suspension by a controlled upward flow. A small particle size (100 – 200 µm) has been employed for the fed-fuels, in order to limit the temperature rise within individual particles.

After each test, fly ashes were collected from both, the tube walls and the ash pot at the bottom of the reactor (Figure 5). The composition of the raw gas (CO, CO_2, H_2O, NO_x, N_2O, SO_2, HCl) was simultaneously monitored during the experiments by Fourier transformed infrared, FTIR (Gasmet DX 4000), and O_2 was determined by a paramagnetic oxygen analyzer (Fuji Electric).

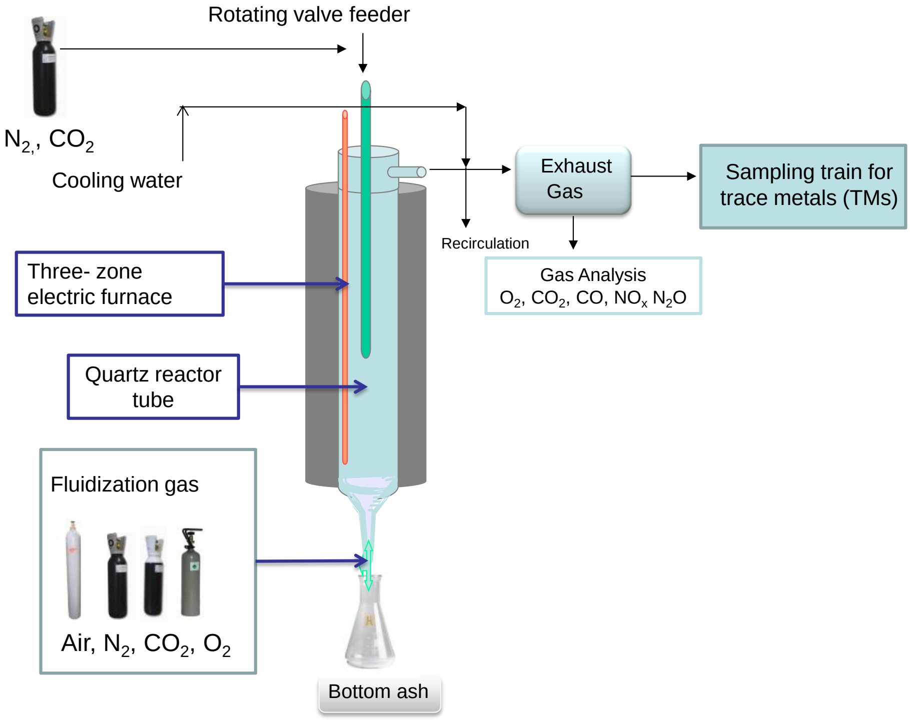

Figure 4. Scheme of the drop tube reactor.

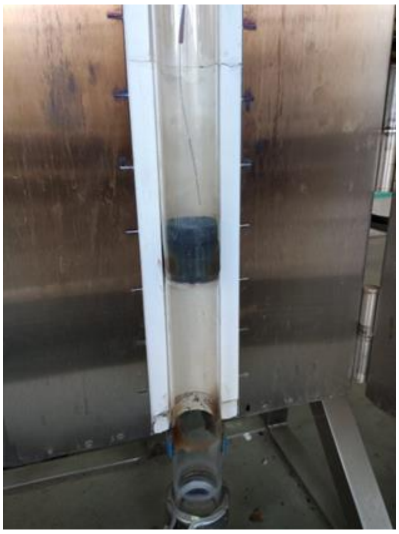

Figure 5. Photo of reactor with ashes after resins are thermally treated.

Table 3 shows the main operational parameters of performed tests.

Table 3. Operating conditions of the thermal treatment.

Fuel	IRN-77, IRN-78
Q, g/h	20 – 25
Fluid	Air
Q fluid, Nml/min	2000
T, ºC	450 – 375
u, cm/s	4,3
Quantity of thermally treated resins, %	15 – 20 %

Figure 6 shows an image of the doped IRN77 and IRN78 resin (left), of the residue obtained after being treated at a temperature of 450 ºC (centre) and of the residue obtained in the crucible after the thermobalance tests (right).

Cationic resin

IRN 77
Doped resin

IRN 77
Thermally-treated waste
450ºC

IRN 77
Ashes
1000ºC

Anionic resin

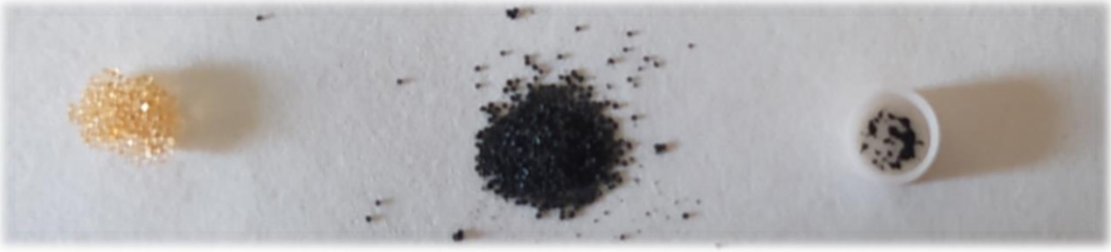

IRN 77
Doped resin

IRN 77
Thermally-treated waste
450ºC

IRN 77
Ashes
1000ºC

Figure 6. Photo of IRN77 and IRN78, thermally treated waste obtained at 450ºC and residue obtained in the crucible after the thermobalance tests (up to 1000ºC).

The main parameters of the particle size distribution of the ashes are shown in Table 4 and Figure 7.

Table 4. Particle size distribution of the ashes after thermal treatment of IERs surrogates.

	IRN 77	IRN 78	IRN77/IRN78 Mix
Mean diameter, µm	470	345	296
Median, µm	459	341	276
Mode, µm	463	346	334
Specific Surface area, m^2/g	0.014	0.023	0.039

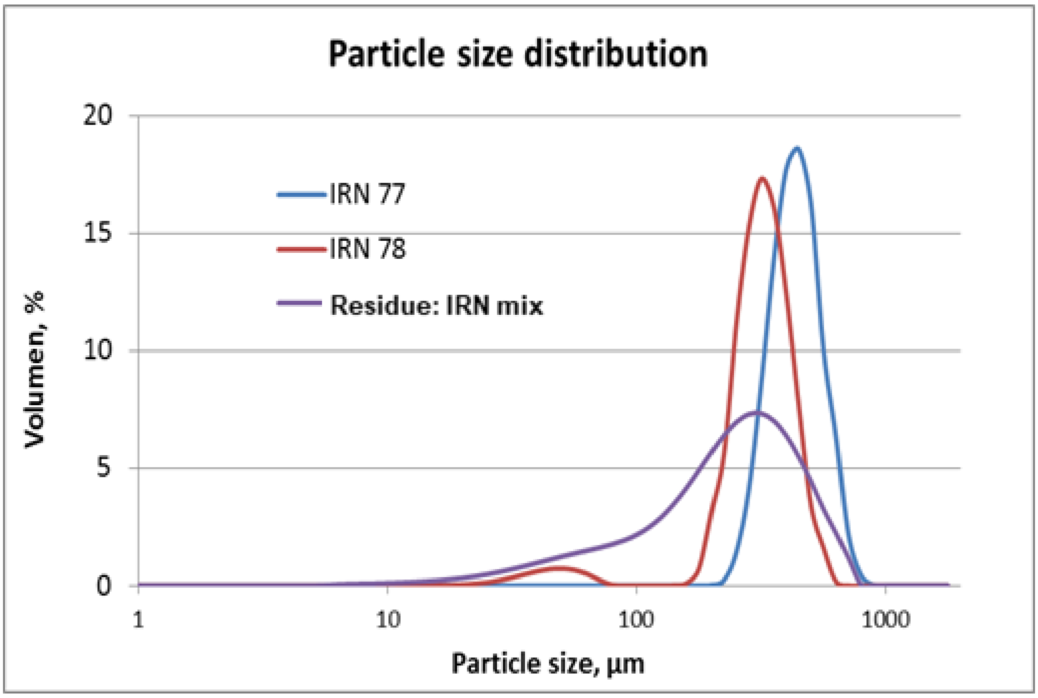

Figure 7. Mean diameter of the ashes after thermal treatment of IERs.

1.4 Characterization of the thermally-treated waste

Main advantages of performing the thermal treatment of the IERs at low-temperature range consist basically of:

- an easier-to-handle product from a radiological point of view, as volume reduction factor is in the range of 4 to 5.
- preventing the loss of volatile elements, such as Cs.

Robustness of the process was also analyzed, as it was considered a key issue to guarantee the representativeness of the obtained thermally-treated waste.

1.4.1 Chemical composition of the thermally-treated waste

Chemical composition of the different batches of thermally-treated waste were determined by means of :

- Chemical elemental analysis (LECO Micro TruSpec)
- A microwave digestion method, using a 7:1 HNO_3: H_2O_2 as digestion solution. ICP-MS analysis was carried out on the resultant solutions (HR-ICP-MS Thermo Fisher Elements).

Average chemical composition of the thermally-treated-waste is shown in Table 5 and Table 6. Chemical composition of the ashes basically consists of a carbon (~ 75%), hydrogen (~ 5%), nitrogen (~ 1%) and sulphur (~ 7%). Trace analysis suggest that no volatilization of minor doping elements have occurred during the thermal treatment of the surrogates.

Table 5. Elemental analysis (C, N, H, S) of IERs surrogates and the thermally treated waste.

	IERs surrogates	**Thermally-treated waste**
Moisture, %	59±3	4±1
Carbon, %	49.0±0.1	74±2
Hydrogen, %	7.1±0.1	5.3±0.2
Sulfur, %	6.81±0.04	7.1±0.5
Nitrogen, %	2.22±0.03	1.21±0.05
Ash, %	< 0,1	< 0,1
C/H	6,9	14,0

Table 6. Boron and trace analysis of IERs surrogates and the thermally-treated waste.

Element	**IERs surrogates**	**Thermally treated waste**
B	5%wt.	16.25%wt.
	mg element/kg	**mg element/kg**
Ca	4,1	17
Co	5	18
Cr	5	18
Cs	30	121
Cu	2	6
Fe	10	40
Mg	1	4
Si	13	48
Sr	4,5	23
Zn	12	48

1.4.2 Structural characterization of the thermally-treated waste

Structural characterization of both, surrogates and ashes, was performed in order to assess the extent of the thermal decomposition of the SIERs. DRX and FTIR spectra are shown in Figure 8 and Figure 9.

From a chemical point of view, thermal treatment of the IERs surrogates can be considered as the combustion of polystyrene copolymers, that are the main constituents of used IERs. XRD analysis of this residue showed that the waste exhibits amorphous characteristics, marked by the presence of an halo in the 10-35 2Θ and another in the 35-45 2Θ. No peaks associated with the presence of crystalline phases were detected. According to FTIR results, ashes are mostly composed of a carbon scaffold with loss of -SO_3 and quaternary amino functional groups during the thermal decomposition of the IERs surrogates.

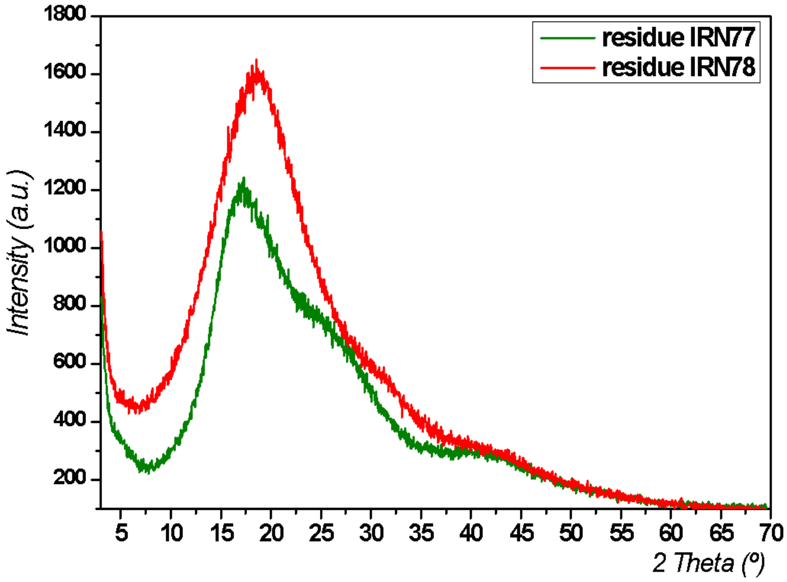

Figure 8. X-ray diffraction pattern of the thermally-treated IERs surrogates .

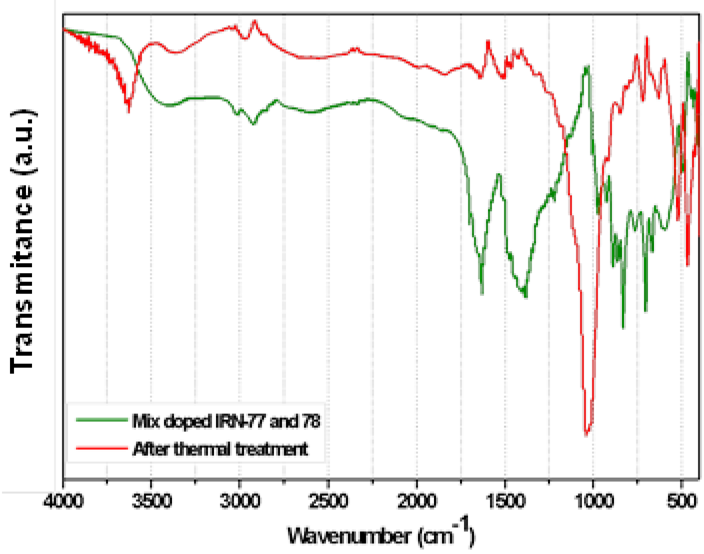

Figure 9. FTIR spectra of the mixture of the IERs surrogates before and after thermal treatment.

SEM observation of the IERs beads after thermal treatment confirmed the granulometry distribution shown in .

Table 4, being the average size observed around 300µm (Figure 10).

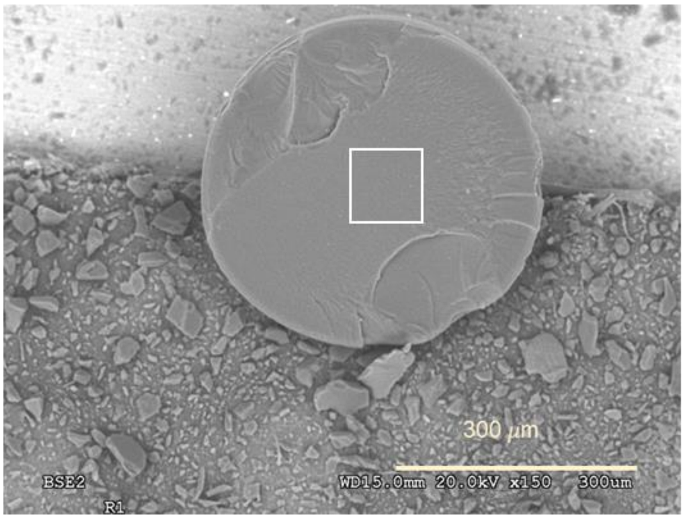

Element	at.%
C	96,16
S	3,54
Al	0,11
Si	0,08

Figure 10. SEM observation and EDS analysis of a cross-section of an IRN-77 particle after thermal treatment.

1.4.3 Behaviour of the thermally-treated waste in alkaline media

Behavior of the thermally-treated waste in a highly alkaline media is another issue of concern for the immobilization and, especially, for the assessment of the durability of the resulting waste package. Aspects like radionuclide or organics release will depend on the long-term stability of the treated waste in a OPC (pH~12) or geopolymer porewater (pH~13) environment.

In order to study stability of the residue obtained from the thermal treatment of the IERs surrogates, two batches of static leaching tests were conducted for 1 and 4 months. Two leachants were used deionized water (as reference) and NaOH 1M in order to mimic a highly-alkaline media expected in geopolymer matrix.

Attending the chemical behavior in solution of the treated waste, these ashes presented an acidic behavior in both water and NaOH 1M. pH values measured in leachates are shown in Table 7.

In order to evaluate the release of organic in the leachant, TOC measurements were carried out in the leachates (

Table 8). TOC in solution was significantly higher in highly-alkaline media than in deionized water. These results seem to suggest that the thermally-treated waste can still undergo some kind of alkaline degradation in highly alkaline media.

Table 7. pH values measured in deionized water and NaOH 1M media after 1 and 4 months.

	pH	
	1 month	4 months
Residue NaOH 1M	11.5	11.6
Residue deionized H_2O	3.4	2.2

NaOH 1 M	13.70
Deionized H_2O	5.8

Table 8. TOC values measured in deionized water and NaOH 1M media after 1 and 4 months.

	TOC mgC/L	
	1 month	4 months
Residue NaOH 1M	109±2	93±4
Residue deionized H_2O	8±2	15±1

1.4.4 Final remarks

For the safe storage and disposal of SIERs, thermal treatment can be an interesting option to avoid problems such as gas and organic complexants generation by radiolysis, cracking of cemented waste forms due to the swelling of SIERs.

Prior to this thermal treatment, removal of the moisture from the IERs is required. Reducing this moisture content is important in order not to excessively penalize the thermal efficiency of the reactor. For this reason, a pre-dehydration step is needed to optimize the energetic balance of the process.

For this project, thermal treatment of SIERs surrogates was conducted in a low-temperature range (375 to 450ºC). Main advantages of treating SIERs at low-temperature (375 – 450ºC) consist basically of:

- an easier-to-handle product from a radiological point of view, as volume reduction factor is in the range of 4 to 5.
- preventing the loss of volatile elements, such as Cs.

Under such operational conditions, resulting product of the thermal treatment of the SIERs surrogates seems to avoid traditional problems associated to the cementation of SIERs. Currently, in the cementation of traditional OPC matrices, swelling of SIERs results in the cracking of cemented drums, limiting the SIERs content in waste packages to a typical range of 12 – 15%wt.

Thermally-treated waste obtained seems to be chemically stable. However, stability in highly-alkaline environments could be an issue of concern and further assessment needs to be carried out in order to guarantee the long-term performance of the reconditioned waste.

2 POLIMI’s contribution: Oxidative pyrolysis and Fenton-like wet oxidation of ion-exchange resins

Contributing authors
E. Mossini, F. Galluccio, A. Santi, E. Rizzi, G. Magugliani, E. Macerata, M. Giola, M. Mariani (POLIMI)

2.1 Treatment of ion-exchange resins

Spent ion-exchange resins produced in nuclear plants and used for the decontamination of radioactive effluents come in huge amount as low-level waste [1]. They comprise a material which is challenging to encapsulate as it stands: it is physically and chemically unstable, and it is incompatible with the inorganic matrices developed so far [2] . Hence, spent IERs are preferably treated to obtain a proper by-product, suitable for conditioning. POLIMI is currently working on two different treatment processes: an oxidative pyrolysis and a Fenton-like wet oxidation. The research activities have also been conducted within 2 M.Sc. theses in Nuclear Engineering (Andrea Santi and Edoardo Rizzi) and 1 Ph.D. thesis in Energy and Nuclear Science and Technology (Francesco Galluccio) conducted at POLIMI.

2.2 Oxidative pyrolysis

The oxidative pyrolysis process was run in batches, mildly heating samples of spent cation-exchange resins in a muffle furnace. The surrogate waste was prepared by contacting pristine beads with aqueous solutions containing at least one of the following stable isotopes of Co, Ni, Sr, Cs, Nd, and Eu, chosen as representatives of fission and activations products, and for their different chemical behaviour. The ashes obtained downstream of the process have been analysed and characterised to assess the possible loss of the contaminants, to measure the achieved reduction of waste mass, and to identify the chemical form. These data are needed to understand the feasibility of their encapsulation in geopolymers.

2.2.1 Outcomes

The investigated thermal process is simple and feasible. It is based on a mild heating of the waste up to 800 °C in air atmosphere. No further gases were employed, nor specific atmospheres are required. The waste was loaded in crucibles with holed lids, to allow exchange of air and minimize dispersion of the waste in the heating chamber. Following the treatment, the waste was retrieved from the crucible, and the latter can be reused for the next batch to reduce the need of decontamination and the generation of secondary waste. Figure 11 reports the scheme of the oxidative pyrolysis.

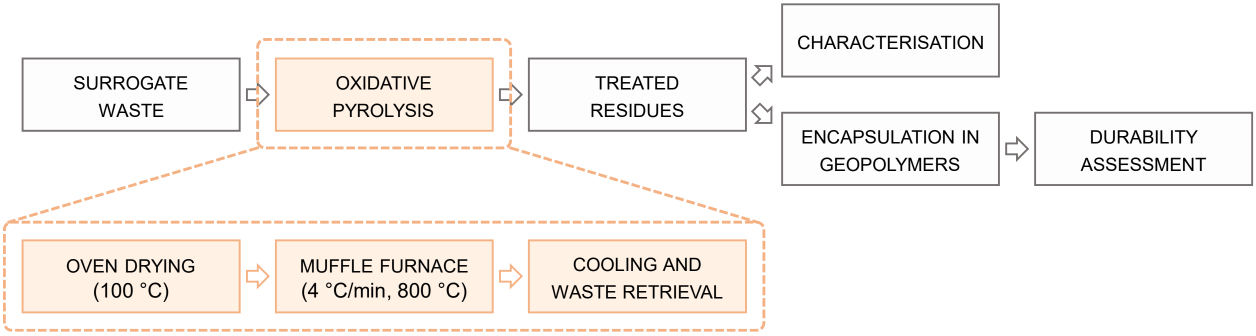

Figure 11. Scheme of the oxidative pyrolysis process.

The heating ramp of the process was designed from to the results available in literature [3,4] and from thermogravimetric analyses run prior to the tests in muffle furnace. Such tests were conservatively performed with resin samples loaded with Cs because of its major volatility [5], and allowed to set the residence temperature as well. An optimal ramp of 4°C/min and an isotherm at 800°C were chosen, aiming at the mild decomposition of the resin beads, to obtain the complete degradation of the organic components, and Cs stabilised as Cs sulphate. Higher values of the heating ramp and of the residence temperature would be responsible for the volatilization of the contaminants during decomposition of the resin beads [4] Hence, the set operational parameters allow to maximise waste mass removal and to minimise the volatilisation of contaminants.

The ashes obtained from the treatment of beads contaminated with one cation at a time comprise sulphates and oxides of the metals (identified by means of Raman spectroscopy and XRD). Both these types of compounds are thermally stable and compatible with encapsulation in geopolymers. No carbon-based residues are identified. Dissolution in concentrated hydrochloric and nitric acid, with subsequent elemental analysis via ICP-MS, proved a retention of contaminants greater than 90%. Figure 12 reports the pictures of the resin samples before and after treatment.

Figure 12. Spent cation-exchange resins: (left) before treatment; (right) after treatment.

For samples simultaneously loaded with the six cations the identification of degradation products via Raman spectroscopy and XRD was not possible because of the chemical complexity of the materials, and only the presence of SO_4^{2-} groups was detected. These residues were harder to dissolve, and a retention greater than 85% was derived for the contaminants. The oxidative pyrolysis of anion-exchange resins is discouraged because of the great volatilization of the contaminated species, which would unavoidably leave the heating chamber and require off-gas abatement systems to avoid their release into the environment.

The reduction of waste mass was derived to depend on the loading factor of the surrogate resin treated and is in the order of 80% for heavily loaded resins. Hence, the process allows to obtain substantial removal of the waste mass, at the same time providing satisfactory retention of the contaminants. The identified phases in the ashes downstream of the pyrolysis are compatible with encapsulation in geopolymers according to a literature overview [6], but this aspect should be experimentally investigated to confirm the overall management strategy.

2.3 Fenton-like wet oxidation

POLIMI has investigated Fenton-like wet oxidation as it is an alternative and green strategy to manage radioactive organic waste such as spent ion-exchange resins [7]. A schematic overview of the process tasks accomplished is depicted in Figure 13.

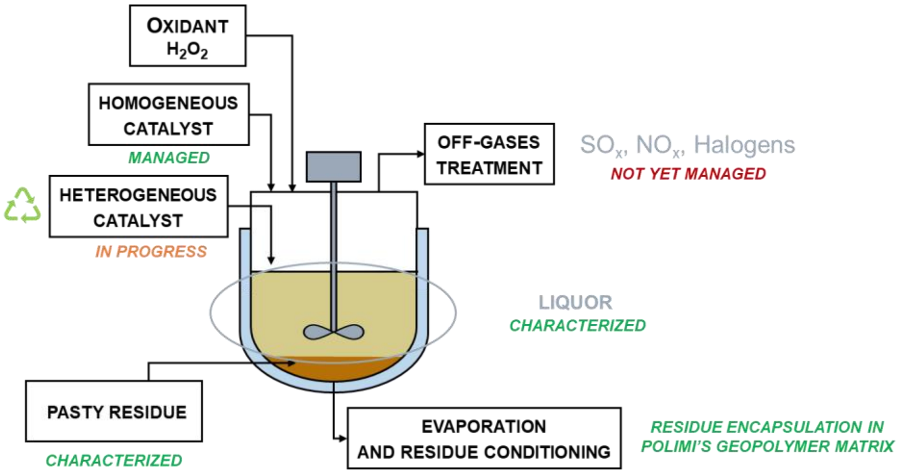

Figure 13. Schematic overview of wet oxidation process and tasks accomplished by POLIMI.

2.3.1 Methods

A surrogate waste was prepared by loading nuclear grade cation-exchange AmberLite IRN77 beads (DuPont) with nitrate salts of stable Co, Ni, Sr and Cs. Anion-exchange resin is AmberLite IRN78 (DuPont) and is doped with KCl and KI salt (Sigma-Aldrich, analytical grade) solutions. The saturation factor with respect to the ion exchangeable resin sites ranges from 10 eq.% to 40 eq.%. Some experiments are performed on cationic resin alone, other with a mixed bed resin.

The experimental set-up shown in Figure 14 comprises a four-necked round-bottom flask, equipped with thermometers and a mixing system, and immersed in a thermal bath to control the reaction temperature of the process at increasing resin batches. A peristaltic pump was used for the oxidant addition into the mixture at controlled flowrate.

Figure 14. Experimental set-up of a Fenton-like wet oxidation process at intermediate laboratory scale (up to 200 g of resin).

The exothermic process was triggered by an iron-containing catalyst and the dropwise addition of an oxidant (H_2O_2). More specifically, two different catalysts have been used to conduct a homogeneous and heterogeneous oxidative process, respectively:

- $FeSO_4$ and $CuSO_4$ aqueous solution;
- Fly ash powder or electric arc blast furnace slag (EA-BFS).

Throughout the process, aliquots of the solutions were collected for further characterisation. Finally, the liquor was recovered and evaporated at the maximum temperature of 70°C. The residue was recovered and stored in sealed containers for further characterisation and conditioning in the tuff-based geopolymer matrix [8].

2.3.2 Homogeneous wet oxidation

Based on a focused literature review and preliminary experimental evidence, the most important process parameters such as temperature, catalyst and oxidant amounts, pH, and reaction time were fine-tuned to control the oxidative process.

2.3.2.1 Cationic resin bed

A small cationic resin batch (10 g) was decomposed in 3 hours. However, a pre-mixing of the resin with the catalyst solution showed beneficial effects with respect to time duration of the process. The temperature profile showed a first reaction peak at 90°C for about 1 hour, then it went down to about 75°C and remained constant for the rest of the process time. The colour change of resin mixture was also used to track the evolution of the oxidative process. The mixture appeared black in correspondence with the peak at 90°C, then it shifted to brown and beyond yellow colour as the organic matter progressively degraded (Figure 15). The mineralization efficiency of cationic resin was assessed by measuring the content of Total Organic Carbon (TOC) as a function of time. The highest value was found within 1 hour close to the reaction peak, then it decreased consistently with temperature profile and colour transitions.

The final mixture was filtered, and an ivory fine precipitate was collected and identified as strontium sulphate by XRD analysis. Downstream of the evaporation process at controlled temperature (< 70°C), a pinkish residue was obtained (Figure 15). So far, characterization of solid phases was conducted by XRD spectroscopy, where mainly inorganic sulphate compounds were identified into the precipitate and residue. Besides, Q-ICP-MS analyses were conducted to monitor cations distribution, and back up the process efficacy.

The successful management of larger cationic resin batches (100 g and 200 g) was the most important step forward in scaling up the process. In this case, the oxidation process required more time to be completed. The scale-up extended the process duration from 3 hours (10 g) to 5 hours (100 g) and towards 8 hours (200 g). The colour of the resin mixture gradually becomes black and the temperature peaks at 95°C. Afterwards, the temperature decreases, the colour progressively fades to brown and becomes yellow in the final phase coherently with what was observed in the small scale of the process.

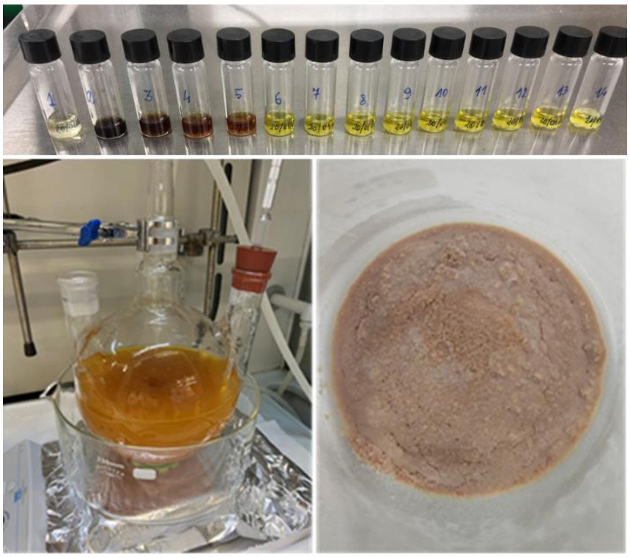

Figure 15. Colour shift of the mixture over time (top), final liquor and obtained residue (bottom).

Overall, a weight reduction ratio (WRR) higher than 60% was obtained for the processes conducted at small and intermediate laboratory scale.

2.3.2.2 Mixed resin bed

The management of a mixed bed resin demanded important adjustments in the operating parameters because of the presence of the anionic resin. For instance, $CuSO_4 \cdot 5\,H_2O$ was added to the $FeSO_4$ – H_2O_2 reaction system as co-catalyst to enhance oxidation of organic matter. Furthermore, a larger amount of oxidant was needed and a longer time duration at increasing mass of surrogate waste was observed, in comparison with an equivalent mass of cationic resin.

The first tests were run to manage a small resin batch (20 g), where monitoring of temperature and colour shift of resin mixture was helpful to understand the evolution of the process. The double-peak reaction showed a great increase in the Chemical Oxygen Demand (COD) when the cationic IER dissolution occurs, while a second broader peak was ascribed to the longer degradation of the anionic IER coherently with temperature profile and colour of the solution. At the end of the process, the COD almost reached the initial value measured before the occurrence of the IER dissolution. Again, a whitish and fine precipitate was found at the bottom of the reactor and identified as strontium sulphate by XRD analysis.

A preliminary scale-up of the process was attempted for the management of larger batches of mixed bed resin (100 g and 200 g). The double-peak oxidative reaction consisted of a first peak at about 90°C, and a second peak at about 95°C representative of the very long decomposition of anionic resin as observed in the smaller scale experiment. The larger scale showed an intense formation of foam because of anionic resin decomposition, and this became more pronounced with a batch of 200 g. Nevertheless, efficacy of the process was promisingly controlled. At the end of the oxidation, more than 95 wt.% of the initial Co, Ni and Cs was found in the resulting liquor, while part of the initial Sr (70 wt.%) was found in the precipitate. On the other hand, ~10 wt.% of I and Cl remains in the final solution since the larger part of them came out as process off-gases. After evaporation stage, a brownish residue was obtained, and characterized by XRD analysis that mainly identified inorganic species like chalcanthite [$CuSO_4 \cdot 5\,H_2O$], iron sulphate [$FeSO_4$], and especially ammonium copper sulphate hydrate [$(NH_4)_2Cu(SO_4)_2 \cdot 6\,H2O$] and ammonium iron sulphate [$NH_4Fe(SO_4)_2$].

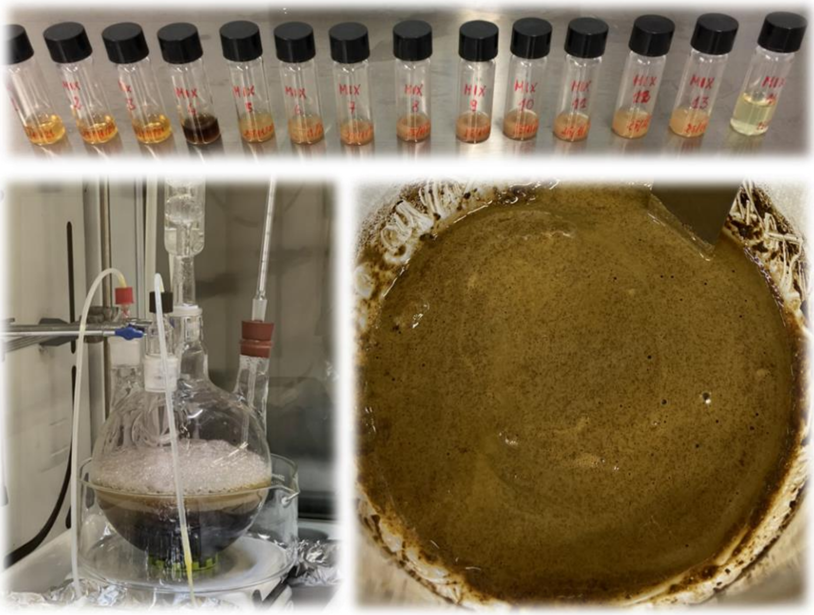

Figure 16. Colour shift of the mixture over time (top). Formation of foam due to anionic resin decomposition and final residue (bottom) in a homogeneous wet oxidation of 200 g of mixed resin bed.

Overall, a WRR of about 80% was obtained for the processes conducted at small and intermediate laboratory scale. In this case, the higher WRR could be ascribed to the co-catalyst effect in the Fenton-like wet oxidation process. On the other hand, the scale-up extended time duration of the process from 3 hours (20 g) to 10 hours (100 g) and towards 15 hours (200 g).

Finally, the residues obtained after the evaporation stage have been encapsulated in the tuff-based geopolymer matrix (Figure 15Figure 16). Compressive strength and water immersion stability at increasing waste loading factor have been investigated. The results will be reported in another document. Beside promising mechanical properties, the specimens loaded with evaporated residues from homogeneous wet oxidation were not durable towards water immersion.

2.3.3 Heterogeneous wet oxidation

During the third project year, POLIMI has been striving to overcome some of the pitfalls arising from homogeneous wet oxidation such as high amounts of sulphates and volumes of the final liquor, strong acidity of the sludge and poor durability of waste forms, by exploring heterogenous Fenton-like wet oxidation based on the recycling of some iron-containing industrial by-products as potential catalysts. Currently, fly ash and EA-BFS are being investigated for the management of up to 100 g of undoped cation-exchange resin. Besides its high Fe-content, fly ash has been selected as catalyst because it is already proficiently employed as precursor in the tuff-based geopolymer encapsulation matrix.

Small and intermediate laboratory scale heterogenous wet oxidation catalysed by fly ash was investigated. Increasing catalyst mass and keeping constant the oxidant flow rate, the single-peak reaction at about 100°C is triggered earlier and lower amount of the oxidant is needed. The evolution of the process was visually inspected by the colour shift and the temperature of the mixture over time (Figure 17).

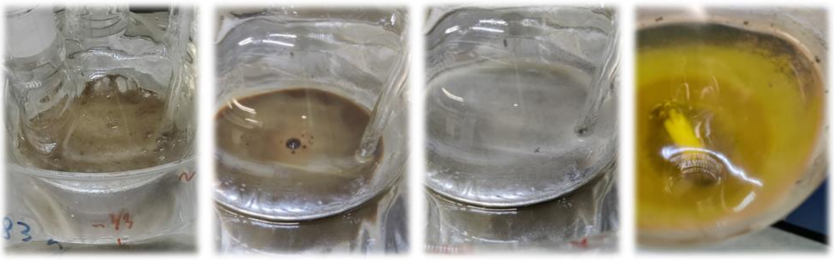

Figure 17. Colour shift of the mixture over time for a heterogeneous wet oxidation conductyed with fly ash as a catalyst at small laboratory scale (10 g of cationic resin).

After evaporating the yellowish liquor, a sludgy residue was obtained (Figure 18). Considering the added catalyst mass, a WRR higher than 60% was calculated for each of the investigated experimental conditions.

Figure 18. Liquors and residues downstream of wet oxidation process by using fly ash (top) and steel slag (bottom) as a catalyst.

An alternative way was found by investigating the use of EA-BFS as catalyst. Similarly, the effect of increasing catalyst mass at constant oxidant flow rate brought the single-peak reaction at lower temperature (96°C) forward. Moreover, the transient response resulted faster than that obtained with fly ash catalyst. The evaporation of the collected liquor resulted in a powdery residue, and a WRR higher than 60% was similarly obtained (Figure 18).

Nevertheless, characterization of the final residues is underway and remains pivotal to properly optimize the process before carrying on with their encapsulation in tuff-based geopolymer matrix.

REFERENCES

[1] Luca, V., *et al*. 2012. *Cation immobilization in pyrolyzed simulated spent ion exchange resins*. Journal of Nuclear Materials 424, 1–11.

[2] Wang, J., *et al*. 2015. *Treatment and disposal of spent radioactive ion-exchange resins produced in the nuclear industry*. Progress in Nuclear Energy 78, 47–55

[3] D. Scheithauer, W. Heschel, B. Meyer, S. Krzack (2017) Pyrolysis of undoped and multi-element doped ion exchange resins with regard to storage properties. Journal of Analytical and Applied Pyrolysis 124, 276-284.

[4] H.C. Yang, S.Y. Lee, Y.C. Choi, I.H. Yang, D.Y. Chung (2017) Thermokinetic analysis of spent ion-exchange resins for the optimization of carbonization reactor condition. Journal of Thermal Analysis and Calorimetry 127, 587–595.

[5] P. Antonetti, Y. Claire, H. Massit, P. Lessart, C. Pham Van Cang, A. Perichaud (2000) Pyrolysis of cobalt and caesium doped cationic ion-exchange resin. Journal of Analytical and Applied Pyrolysis 55, 81-92.

[6] Ahn. J, *et al*. 2019. *Development of metakaolin-based geopolymer for solidification of sulfate-rich HyBRID sludge waste*. Journal of Nuclear Materials 518, 247–255.

[7] S.A. Walling, W. Um, C.L. Corkhill, N.C. Hyatt, Fenton and Fenton-like wet oxidation for degradation and destruction of organic radioactive wastes, Npj Mater. Degrad. 5 (2021) 1–21. https://doi.org/10.1038/s41529-021-00192-3.

[8] A. Santi, E. Mossini, G. Magugliani, et al. “Design of sustainable geopolymeric matrices for encapsulation of treated radioactive solid organic waste”. Frontiers in Materials 9, p. 1-17 (2022). DOI: https://doi.org/10.3389/fmats.2022.1005864

3 Thermal gasification by SIIEG

Contributing authors

Yu. Zabulonov, B. Zlobenko, A. Pugach, A. Rozko, Yu. Fedorenko, SIIEG

When decommissioning nuclear facilities, it is necessary to process large volumes of radioactive waste, an industrial problem. Over the past few years, there have been several innovative projects to develop specific heat treatment processes [9-11]. The literature broadly describes studies of the low-temperature pyrolysis of spent IERs. An earlier study by Matsuda et al. investigated the influence of the functional sulfonic acid group on the pyrolysis characteristics of cation exchange resins [12]. These studies focused on the pyrolysis conditions that allow the retention of radioactive elements in a pyrolysis residue. The papers studied low-temperature pyrolysis of spent ion-exchange resins in a pebble bed at approximately 500°C with keeping radioactive cesium species in the solid pyrolysis residue [13, 14], have led to valuable reductions in waste volumes.

3.1 Description of work

The decomposition of IER by thermal gasification results in significant volume reduction, which was demonstrated successfully in many projects. The State Institution “Institute of Environmental Geochemistry” NASU (IEG) research group with partners has worked for several years to develop a hybrid process of gasification of IER and has designed new and innovative equipment for safe and efficient deep processing of thermal treatment of the RSOWs, with obtaining useful energy products (electricity, hot water, heating). The system for the thermal treatment of radioactive waste consists of a thermal treatment unit with a plasma torch and gas cleaning technologies, a heat exchanger, and a control unit (Figure 19).

The thermal treatment unit consists of a hopper for loading waste, a gasification chamber, a gas afterburner, a heat exchanger, and a smoke exhauster. The lining is made of high-temperature ceramics.

Figure 19. System for thermal treatment based on gasification technology.

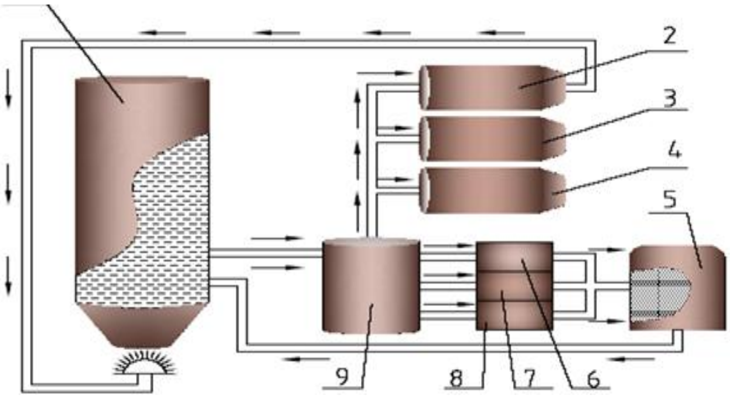

Figure 20. The multiloop circulation gasifier system.

In figure: 1 - reactor, 2 - output circuit gaseous compounds, 3 - closed circuit solid compounds, 4 - output circuit for the solid residue, 5 – a unit of catalyst, 6,7,8 - sectional contours, 9 - Multiloop coolant distribution unit

The multi-loop circulating gasifier is a fundamentally new technology that provides a complete thermal decomposition of solid radioactive organic waste at high temperature in the reactor (1) without oxygen access (Figure 20). Toxic components formed in the form of a gas mixture circulate in a multi-circuit system (5, 6, 7, 8, 9) until complete decomposition to low molecular weight components. The resulting pyrolysis gas (2) has burned in a device that prevents toxic elements formation.

3.2 Materials

The primary material used in this study is KU-2-8 cation exchange resin supplied by the VAT "AZOT", GOST 20298-74. The resin consists of sulfonic acid groups ($-SO_3H$) and an insoluble skeleton formed by copolymerisation of styrene and divinylbenzene. The surrogate waste with stable Cs of the cation-exchange resin was used for loading. The initial moisture content of the resin was up to 65% wt. Drying was carried out until the moisture content of the resin reached 5 – 15% wt. Gasification of the IER was initially determined through a kinetic analysis by a DTA study. The process has been carried out at temperatures of 650 – 850°C (Cs_2SO_4 $T_{melting}$= 1019°C; $T_{boiling}$ =1900°C)

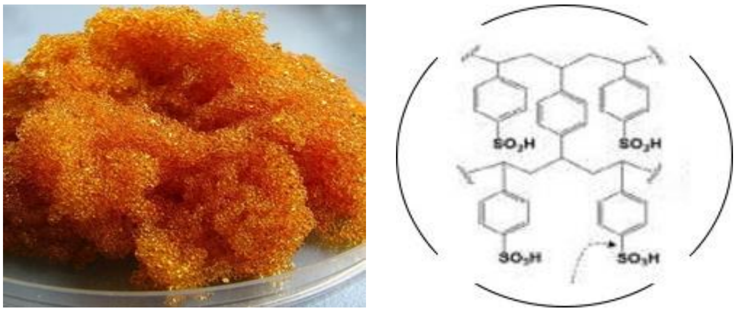

Figure 21. Cation-exchange resins KU-2-8.

Cation-exchange resins represent spherical granules of high-molecular polymeric compounds (styrene-divinylbenzene copolymer) with gel structure. The diameter of granules is 0.315 – 1.25 mm. The following resin grades were used at ChNPP: KU-2-8 and their analogues. This waste is classified as low-, and intermediate-level LRW. Volumes of Ion-exchange resin - 4 077 m^3. The cation-exchange resin (KU-2-8) was used for experiments.

3.3 The main steps of processing IER

The initial stage of thermal utilization of radioactive waste is when the processing system reaches operating mode. Using a gas burner, the recovery chamber is heated to a temperature of 850°C. Processing at a temperature of 800°C occurs with partial sintering of the IER. DTA examined the resulting ash for the study of velocity decomposition. The recycling chamber is stable - the recycling process begins, and we supply 0.5 kg IER waste has started the heat treatment process. The treatment process was 50 – 70 minutes. After cooling the bottom chamber, we extract the ash in quantity 82 grams.

Ecological safety is the primary requirement imposed on modern technological processes of Radioactive Solid Organic Wastes processing. Adopting the multiloop circulation gasifier principle in waste processing allows fulfilling this requirement for the major part because of the more profound destruction of wastes. As a result, toxic high-molecular components are transformed into low-molecular ones, reducing their toxicity. Furthermore, toxic volatiles in the pyrolysis gas are after-burned at a temperature of 1100 – 1400°C, which provides dioxins and furanes to decompose entirely.

Disadvantages of gasification

- Gasification of heterogeneous polymeric and organic radioactive waste leads to a heterogeneous composition of the generated syngas, which forces the design of complex control systems for energy converters;
- Ignition and maintenance of the desired temperature in the gasification zone with heterogeneous waste is very difficult;
- To obtain acceptable overall dimensions, it is necessary to increase the thermal stress of the gasifier housing.

3.4 Process of steam-plasma gasification feasibility

There have been many studies of conventional thermal treatment technologies such as incineration and other similar processes, which combust or gasify most organic constituents to final ash and have led to a very large volume of off-gas bearing unburned hydrocarbons, toxic, acid gases and vaporisation of radioactive elements. To solve the problems associated with the shortcomings of gasification, the most promising approach is plasma technologies. Plasma heat generators in systems for the thermal treatment of various wastes are more efficient due to the ability to reach high temperatures of the processing process, sufficient for the destruction of any organic substances and the complete melting of all inorganic materials with a high degree of control of the thermal regimes of the process. This allows plasma technology to process waste and produce stable, harmless end products. At the same time, multiple reductions in the volume of waste (up to 95%) are achieved, and the resulting solid residues contain concentrates of all harmful waste components in a bound, safe state.

Figure 22. The installation trials of plasma torch gasification.

This work proposes a novel for spent IER conducting a two-stage process of the carbonisation of organic constituents and high-temperature plasma.

The thermal treatment plant consists of a waste loading bin, a gasification chamber, a gas afterburner, a heat exchanger and a smoke exhauster (Figure 20). The lining is made of high-temperature ceramics and the heat exchanger is made of stainless steel (Figure 22). Plasma technologies require unique refractory lining materials which are durable to the extremely high temperatures and aggressive influence of the residue ash (slag). The construction of a high-temperature reactor has provided the most effective heating slag and prevented excessive heat losses. The experiments were carried out using a plasma torch with a reactor with a spatially developed active zone.

Steam plasma gasification does not lose its destructive efficiency with a change in the moisture content of the IER. In the work of Dobrohotov N. N. [15], three defining reactions for the main process are considered:

- the furnace at the bottom of the generator

  $C + O_2 + 3.8\ N_2 = CO_2 + 3.8\ N_2 + 97{,}650$ cal;
- decomposition of carbon dioxide in the next highest level of the generator

  $C + CO_2 \leftrightarrow 2CO - 38{,}800$ cal;
- decomposition of water vapour by hot carbon in the level water gas reaction

  $C + H_2O \leftrightarrow CO + H_2 - 28{,}400$ cal.

An essential gasification problem is the completeness of thermal treatment, which allows removing organic substances from IER without releasing large amounts of radionuclides. Fundamental experiments have refined the pyrolysis characteristics of cation-exchange resins. Introducing the principle of a multi-circuit gasifier in waste processing gives more profound destruction of waste, reducing the amount of waste with the accompanying decomposition of organic matter. As a result, toxic high molecular weight components have transformed into low molecular-weight ones, thereby reducing their toxicity. In addition, toxic volatile substances present in the pyrolysis gas are afterburner at a temperature of 1100 – 1400°C, which ensures the complete decomposition of dioxins and furans.

The steam-plasma process provides highly efficient, environmentally friendly processing of organic waste without the emission of such harmful substances as dioxins, resins, phenols, and aerosols into the environment. It is the production of the target product in the form of synthesis gas, which is a valuable energy carrier, as well as safe, solid products of processing, suitable for further conversion into material stable for long-term burial.

Vapour-plasma conversion provides complete thermal and concentration uniformity throughout the workspace. During the entire processing time, due to the high transport properties of steam, all surface elements of the solid and liquid phases are in the same thermodynamic conditions. This ensures the guaranteed processing of materials in the entire volume of the reactor.

The process of steam-plasma gasification is insensitive to the humidity of the processed waste. It retains destructive efficiency with changes in the moisture content of the solid. In processing, dangerous elements such as chlorine, fluorine, etc., part of many plastic materials, are bound and easily removed. During the gasification of carbon-containing substances with water vapour at high thermodynamic parameters, there are no sulfur compounds in the gas phase - it entirely remains in the solid residue (slag). Steam plasma torches (steam plasma generators) have a significantly higher service life than traditional ones. The equipment is compact and reliable.

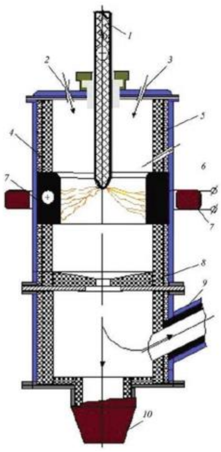

1 - graphite electrode (cathode);

2 - branch pipe for IER input;

3 - branch pipe for introducing water vapour;

4 - graphite filling;

5 - graphite lining;

6 - annular graphite electrode (anode);

7 - electromagnetic coil;

8 - graphite diaphragm;

9 – synthesis gas outlet pipe;

10 - slag outlet pipe

Figure 23. Schema of the plasma torch reactor.

The gasification technology using a plasma torch system using steam was the most efficient and preferred for this process. Unlike other systems, vapour-plasma gasification makes it possible to effectively ash IER, control the process temperature, and safely burn gases without the possibility of leakage of radioactive materials.

The initial stage of thermal utilisation of organic radioactive waste is entering the processing system into operating mode and loading it into the bunker. Bunker with radioactive waste with humidity up to 80% preheated with a gas burner, and the heat treatment process starts. Hot water has supplied to the air convectors' heating system. A smoke exhauster controls the process of removing gases. After gasification, ash has removed from the system and loaded into special steel containers for further sealing. The dimensions of the crucible play an important role. The most efficient treatment is achieved in a long crucible with a small diameter. This design allows you to heat and ash the contents of the crucible evenly (Figure 25). The experiments have carried out using a plasma torch with a reactor with a spatially developed active zone. Temperature 1200 – 1250°C for the plasma gasification to take below the boiling point of Cs_2SO_4, which allows it to remain in the ash. The absence of ballast nitrogen and free oxygen in the reaction chamber eliminates the problem of the formation of nitrogen oxides, which ensures the high quality of the resulting synthesis gas and does not require additional measures for its separation and purification. An essential gasification problem is the completeness of thermal treatment, which allows removing organic substances from IER without releasing large amounts of radionuclides.

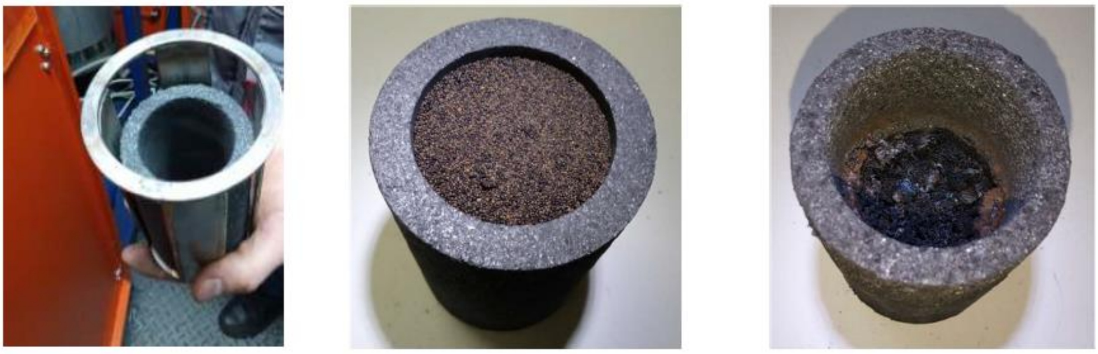

Figure 24. Ion exchange resin treatment process.

According to the experimental conditions, 2 kg was loaded IER into the crucible. Gasification technology is operated in two stages and consists of reactors operating in the temperature range from 800 to 1250°C. Processing time 90 – 120 minutes. A feature of this process is reaching the reactor mode and maintaining the temperature regime for a long time. The experiments were carried out using a plasma torch with a reactor with a spatially developed active zone. As a result of heat treatment, we have ash and a decrease in weight of IER waste up to 300 – 350 grams.

TECHNICAL SPECIFICATIONS

Thermal pyrolysis:	High temperatures and decomposed without oxygen
Heating method:	By clashes and friction of matter parts
Treatment cycle duration:	About 120 minutes
Nominal waste loading potential:	50 – 250 kg waste/hour with 80% humidity
Treated material aspect:	Different organic wastes
Treated material final volume:	About 0,5% of the initial volume
Treatment cell volume:	About 330 litres
General control system:	Programmable logic controller (PLC)
Temperature measurement:	By sensors
Cycle recording:	Time/temperature variation recording

The phases of the primary cycle and the installation parameters are displayed on the LCD panel during the execution of the cycle. The main physical parameters of the process (e.g. temperature, pressure, time and gas composition) are controlled. The control system is easy to use as the plant control is programmable. The automatic operating system (automatic cycle selection) for the entire cycle guarantees maximum safety. During the experimental work, a surrogate waste cationic IER has used for loading. Processing occurs with the sintering of the IER ash Synthesis gas, solid residue, and gaseous compounds are dependent on thermodynamic parameters and process speed.

Figure 25. System for thermal treatment of the radioactive wastes based on gasification technology with a plasma reactor.

Gasification technology is operated in two stages and consists of reactors operating in the temperature range from 600 to 1250°C. The temperature control in the reactors is separate and allows for setting different temperatures in each reactor. The role of the second stage is often variable but basically complements the first one and is mainly used for the high-temperature oxidation of flue gases with a high content of carbon monoxide and hydrocarbon residues and the capture of fly ash containing radionuclides. To achieve optimal oxidation, the temperature must be above 800 °C, and it is preferable to operate the reactor with at least 900°C to reduce the necessary residence time of the reactants in the reactor.

3.5 Research Outlook

This study demonstrated that gasification of the IER would be beneficial to reduce the total volume of LILW requiring predisposal treatment. Thus, the thermal treatment process uses a plasma torch with a multi-loop circulating gasifier that provides a complete thermal decomposition of organic radioactive waste without access to oxygen at high temperatures. Synthesis gas, solid residue and gaseous compounds depend on thermodynamic parameters and process speed. Under an experimental test, inactive ion exchanger surrogates demonstrated this process's capability to remove radionuclides from spent IER. Waste gas products were monitored in experiments. In this case, directive 2000/76 /EC [16] determines their requirement.

3.6 Characterisation of ashes from thermally-treated RSOW by IEG process

Reducing the volume of radioactive spent IERs is one of the complex problems for nuclear industries. Available treatment approaches include direct and after thermal decomposition [15, 18], solidifying this waste to suitable forms for storage/disposal. The incineration for the treatment of radioactive IERs encounters the challenge of off-gas treatment (e.g., ^{137}Cs, SOx, NOx) and would face further ash/slag treatment problems. The influence of the functional sulfonic acid group on pyrolysis characteristics for cation exchange resin was investigated with the last centennial.

The paper [19], investigated the pyrolysis characteristics of the cation resin by thermogravimetric analyses and residual elemental analyses. When examining the highly acidic cationic resins with a sulfonic group, he found microporosity created during heat treatment. As the temperature rises, the volume of micropores increases, and the adequate size of the micropores decreases. The micropore volume increases linearly as the skeletal volume decreases, with half the volume lost by the skeleton creating new micropores and the other half appearing as shrinkage of the bead. As shown, pyrolysis with the flow of nitrogen indicates that even after pyrolysing from room temperature to about 900°C, a significant mass fraction of the original cationic resin remains, approximately 46%.
Studies reported by Matsuda et al. [19] concluded that after pyrolysis of spent ion exchange resin, residual elemental analyses, and off-gas analyses, the decomposition ratio of cation resins was only 50 wt % at 600°C. In contrast, that of anion resins was 90 wt% at 400°C. Infrared spectroscopy for cation resins attributed its low decomposition ratio to forming a highly heat-resistant polymer (sulphur bridged) during pyrolysis. In the paper [21], the pure IER is pyrolysed at different temperatures, and XPS analyses the solid residues, and the results are shown in Figure 26.

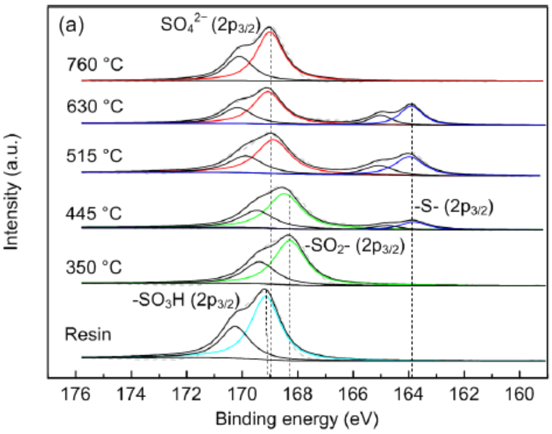

Figure 26. XPS spectrums of pyrolysis residue at different temperatures of pure resin [21].

As shown in Figure 26, S2p exhibits four peaks in XPS spectrums of residue, located at 169.1 eV, 168.9 eV, 168.2 eV, and 163.8 eV, representing the sulphonic acid group ($-SO_3H$), sulphate sulfur ($-SO_4^{2-}$), sulphone sulfur ($-SO_{2-}$), and organic sulphur bond (-S-), respectively. As shown in Figure 26, the $-SO_3H$ in the raw resin is first converted to $-SO^{2-}$ at 350°C, then partial $-SO^{2-}$ transforms into $–S_{-}$ at 445°C. At 515°C and 630°C, the sulphur is mainly present in SO_4^{2-} and $-S^{-}$. Finally, $-S^{-}$ completely decomposes, and the form of sulphur in the pyrolysis residue is mainly SO_4^{2-} at 760°C.

3.6.1 Physical and chemical characterization of thermally-treated IERs surrogates

This work aimed to investigate the application of a geopolymer binder to ash/slag after IER gasification and the problems associated with ash requirements. First, the assessment of factors critical to the performance of geopolymer grouted. Ash usually contains several weight per cent of sulphur (VI), shown in Table 9, the chemical analysis of ash. However, even the low sulphide sulphur content in slag dominates the redox effect. The reaction between sulphur(VI) and sulphide ($S^{2–}$) causes intermediate sulphur species to form, specifically thiosulfate ($S_2O_3^{2-}$).
To quantitatively characterise the change of the $-SO_3H$ and the copolymer matrix during the IER pyrolysis process, the solid residues were subjected to elemental analysis, and the results are presented in Table 9.

Table 9. Ashes characterisations by chemical analysis.

Component	C	S	Cs
%weight	72,4	2,8	2,1

Interactions between the ash components and the geopolymer grout can affect the matrices' setting, hardening, and strength development. As treated IER ashes came at different temperatures, research on ash waste was carried out. A significant gasification problem is the completeness of thermal treatment, which allows removing organic substances from IER without releasing large amounts of radionuclides. The ion exchange resin combustion method is optimised by determining the temperature of the gasification process for the gradual conversion of mobile and volatile Cs species into inorganic and thermally stable compounds.

3.6.2 Experimental materials

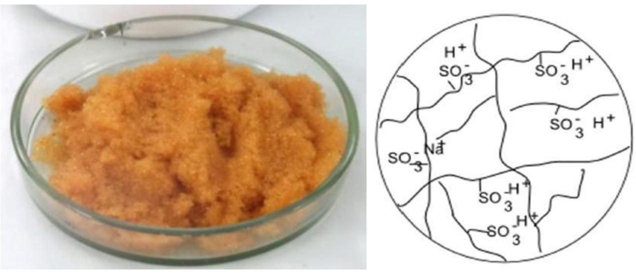

Figure 27. Chemical structure of the strong acidic cationic ion exchange resins with functional groups of –SO_3H^+.

Ion-exchange resins represent spherical granules of high-molecular polymeric compounds (sulfonated polystyrene-divinylbenzene copolymer) with gel structure. Ion exchangers generally comprise cross-linked polystyrene (Figure 27) to which functional groups are added for ion exchange purposes: sulfonyl groups -SO_3H for cation exchangers. The diameter of granules is 0.315 – 1.25 mm. The following resin was used at Chornobyl Nuclear Power Plant (ChNPP): КУ-2-8, which contains fixed ions - sulphogroup -SO_3H (H-form of a resin) or KA-11 (-SO_3Na, Na- form resin) and their analogues. This waste is classified as low-, and intermediate-level LRW. Volumes of spent ion-exchange resin at ChNPP - 4 077 m^3.

3.6.3 Characterisation of the ash

Due to the strong dependence of carbon content in the ash on the condition and temperature of IER waste gasification, one of the main goals was to characterise the ash phases and link this information to their behaviour under solidification. When heated by the IER, the particles separating decrease in size. It was established that at a temperature of about 600°C, the particles, at the same time, sintered into aggregates. At a temperature of about 600°C, due to the cracks, IER, the fragments are separated from the original, and, at the same time, the particles are sintered into 5 – 10 mm in size aggregates. In the future, cracking continues while the particles oxidise (Figure 28).

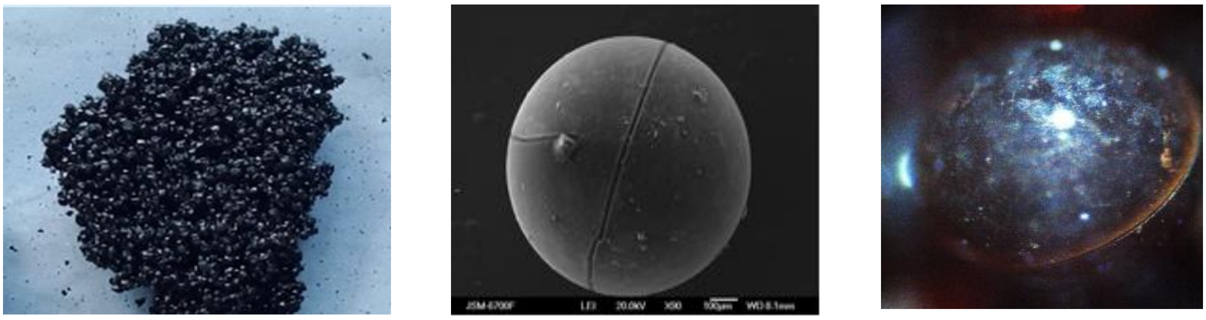

Figure 28. Snapshot of ash after thermal processing at 400°C.

The original ash samples were fractionated by sieving. The fractions collected were characterized and used in the experiment. The cationic IER is characterised by releasing more significant quantities of a degradation product, mainly SO_2. In the article Matsuda the lower mass reduction of the cationic IER to the stabilisation processes of the residual matrix associated with the formation of sulphur structures [21]. The main constituent of the product, the ash, is carbon.

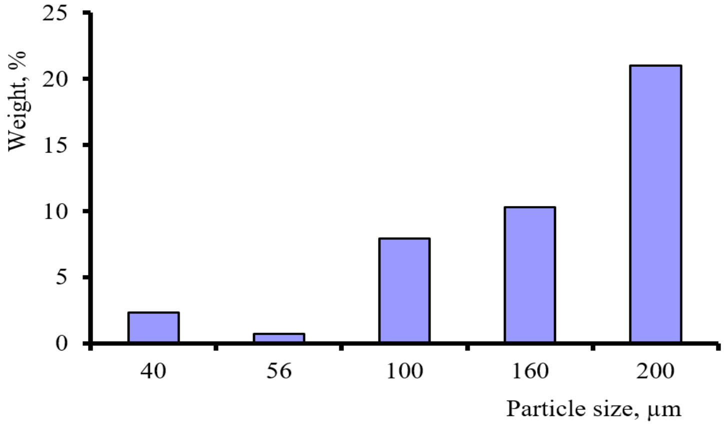

Figure 29. Size distribution in the fraction < 0,3 mm particles ash after burning 87% of the IER.

Incineration of significant volumes of spent ion-exchange resins can be problematic, also taking into account the uncertainty of the behaviour of the temperature and duration of gasification. The resulting ash was characterised using FTIR spectroscopy, SEM, and DTA to monitor the decomposition level of IER organic matter. Previously, it was established by the DTA method that with a small mass of the sample, it is wholly heated with a minimum temperature gradient over the sample volume.

3.6.4 Scanning electron microscopy

The thermal degradation samples of IER were studied by examining the surface morphology of resin samples heated using the JSM-6490LV Scanning Electron Microscope (Jeol Ltd., Japan). In Figure 30, the sequence of destruction of spherical particles of the cation IER during heat treatment is given. When heated, the particles of an IER crack from them, separating scales, and they decrease in size. At 400°C, the resin showed cracks in the spherical structure, which supports the breaking of the polymer matrix at that temperature. In the future, cracking continues while the scales begin to burn out. At sufficiently high temperatures, particles of a spherical shape can be preserved in the samples. The presence of such particles in the samples significantly reduces the ultimate compressive strength of the geopolymer matrix; reducing their number in the samples of compounds is an urgent problem and requires a higher temperature after the first gasification.

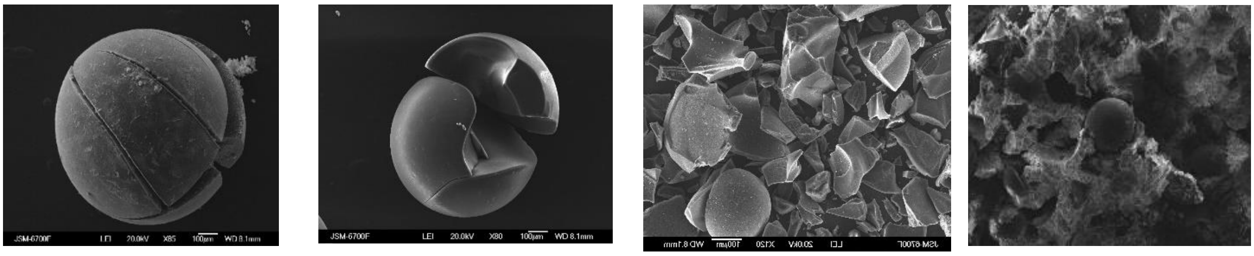

Figure 30. Destruction of IER under gasification.

From Figure 30, it can be seen that IER particles are of different sizes. SEM photographs of resin at 700°C show complete cracking of the spherical structure, and because of the difference in size, smaller resin species got inserted into the larger broken spheres.

3.6.5 DTA analysis

The DTA analysis was performed on a Q1500D (MOM, Hungary) thermal analysis system between 20 – 1000°C. Figure 31 represents a weight loss of an IER from room temperature to 1000°C under a nitrogen atmosphere. Between 100°C and 200°C, the weight loss is to dehydration. The major mass loss starts at 400°C (Figure 31). In the temperature range of 400 – 800°C, degradation products' weight loss and volatilization occur rapidly. According to the studies of the thermal behavior of the sulphonic cationites [22], the decomposition steps are as follows: dehydration, destruction of the functional groups by SO_2 elimination, and oxidative degradation of the polymeric matrix. The last decomposition step between ~800°C and 1000 °C corresponds to the total degradation of the IER matrix and of the ash fragments.

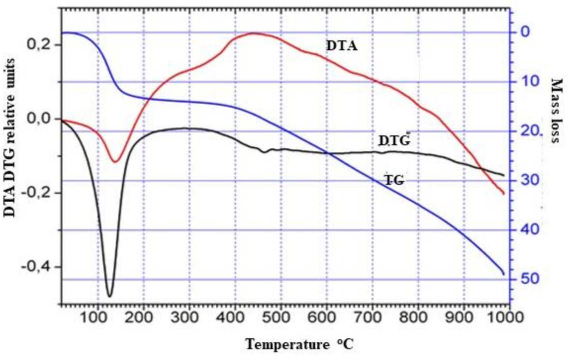

Figure 31. DTA analysis of samples of IER.

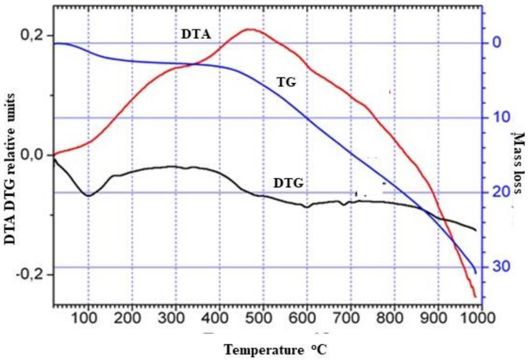

Figure 32. DTA analysis of samples of ash

On the Figure 32 represents repeated studies an ash, which showed that complete decomposition (99%) could occur at a temperature of 1000°C.These analyses suggest that the degradation of IER can be separated into three primary stages: weight loss between 25 and 150°C is ascribed to dehydration. Most weight loss results from decomposing the functional groups from 250 to 800°C for cationic exchange resins. The last stage (temperatures from 800°C) is associated with degrading the particle's organic matrix and its subsequent mineralisation.

3.6.6 FTIR spectra

To make clear the steps in the production of ash compounds, FTIR spectra of the cationite ash have been recorded. FTIR spectra (the 4000 – 400 cm^{-1} range) of thermally decomposed samples were recorded in KBr pellets (2 mg ash/200 mg KBr) using FTIR Thermo Nicolet Nexus spectrophotometer.

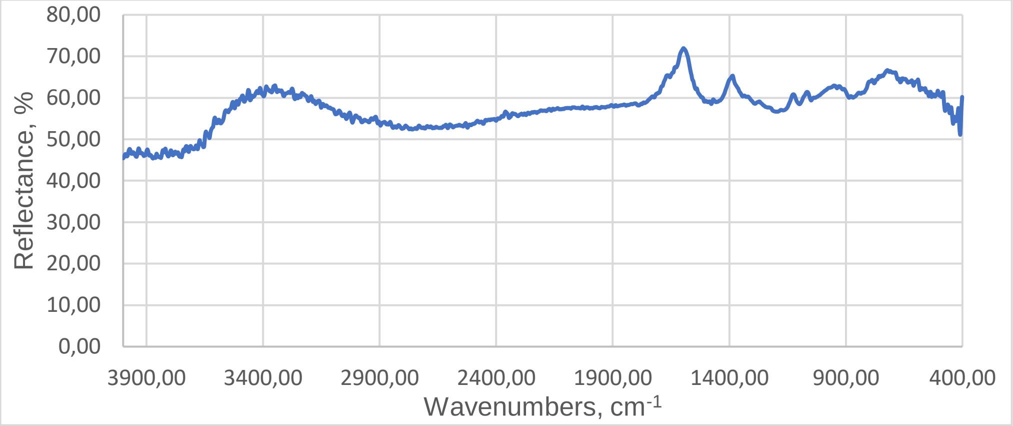

Figure 33. FTIR spectral analysis of the IER ash in the 4000 – 400 cm^{-1} region.

FTIR spectral analysis of the IER ash in the 4000 – 400 cm^{-1} region shows stretching vibration bands at 1064 and 1126 cm^{-1}, corresponding to the functional group of sulphonic acid ($-SO_3H$). The S–O stretching vibrations at 705 cm^{-1}, skeletal vibration band aromatic nucleus C=C at 1599–1604 cm^{-1}, indicating unburned resin. The wide band of stretching vibrations of O–H hydrogen bonds at 3200 – 3500 cm^{-1}. At 400°C, the IR study shows that the peaks in the 1500 – 1000 cm^{-1} region either have a general broadening or disappear. sulphonic parts of the ring. The band is observed at 1612 cm^{-1} for the C=C aromatic bond, which remained unchanged.

Asymmetric stretching of SO_2 at 1384 cm^{-1}. Two sharp peaks at 1064 cm^{-1} and 1126 cm^{-1} are due to the symmetrical stretching of SO_3. Bands appear at 2366 cm^{-1}, which can be attributed to O–H stretching vibrations originating from hygroscopic water. Due to sulfur groups' symmetric and asymmetric stretching vibrations, bands between 1000 cm^{-1} and 1200 cm^{-1} are observed in the spectrum. However, at higher temperatures above 800°C, most functional sulphonic acid groups decompose with the release of SO_2.

3.6.7 Conclusion

During the experimental work, a surrogate waste cationic IER has used for loading. Processing occurs with the sintering of the IER ash. Methods of DTA, SEM, and XRF to study decomposition and the resulting ash. Solid residue (ash) is dependent on thermodynamic parameters and process speed. The thermal degradation study of acid ($-SO_3H+$) cationic IER shows a slight mass loss of 55% up to 900°C. The slight weight loss of acid IER was attributed to forming of sulphonyl and sulphur bridges between base polymers after the dehydration reaction.

REFERENCES

[9] Nieminen M. et al., Gasification-based thermal treatment of Low and Intermediate Level Waste containing organic matter IOP Conf. Ser.: Mater. Sci. Eng. 818 012007, 2020

[10] Neubaer J., “Incineration of ion-exchange resins: operational experience” Proc, of 1996 Int. Conf, on Incineration and Thermal Treatment Technologies, Savannah, Georgia, USA, pp.239-241, 1996

[11] Neely, J. W. Characterization of Polymer Carbons Derived from Porous Sulfonated Polystyrene, Carbon, 19, 27, 1981

[12] Matsuda M., Funabashi K., and Yusa H., Influence of Functional Sulfonic Acid Group on Pyrolysis Characteristics for Cation Exchange Resin, Journal of Nuclear Science and Technology, 24, 2, pp. 124-128, 1987

[13] Tang H, Xu M, Hu Hy, et al., In-situ removal of sulfur from high sulfur solid waste during molten salt pyrolysis. *Fuel*, 231:489-49, 2018. https://doi.org/10.1016/j.fuel.2018.05.123

[14] Singare P., Lokhande R., Madyal R. Thermal Degradation Studies of Polystyrene Sulfonic and Polyacrylic Carboxylic Cationites. Russian Journal of General Chemistry, Vol. 80, No. 3, pp. 527–532, 2010

[15] Singare P., Lokhande R., Madyal R. Thermal Degradation Studies of Some Strongly Acidic Cation Exchange Resins. Open Journal of Physical Chemistry, 1, p.45-54, 2011.

[16] Directive2000/76/EC of the European Parliament and of the Council of 4 December 2000 on the incineration waste // Official Journal of the European Communities L 332, 28/12/2000. — P. 91–111.

[17] Wang JL, Wan Z, 2015. Treatment and disposal of spent radioactive ion-exchange resins produced in the nuclear industry. Progress in Nuclear Energy, 78:47-55. https://doi.org/10.1016/j.pnucene.2014.08.003

[18] Nieminen M. et al. Thermal treatment for radioactive waste minimisation, EPJ Nuclear Sci. Technol. 6, 25 (2020) , https://doi.org/10.1051/epjn/2019040

[19] Matsuda M., Funabashi K., and Yusa H., Influence of Functional Sulfonic Acid Group on Pyrolysis Characteristics for Cation Exchange Resin, Journal of Nuclear Science and Technology, 24, 2, pp. 124-128, 1987

[20] Jung, H.G., Brähler, G. & Slametschka, R., Pyro(hydro)lysis of Spent Ion Exchange Resins for Disposal of Organic-Free Radioactive Waste. IGD-TP 7th Exchange Forum, October 25-26th, 2016, Córdoba, Spain, 2016

[21] Georg, B.; Rainer, S. Pyrolysis of spent ion exchange resins. In Proceedings of the Nuclear Plant Chemistry Conference 2012 (NPC 2010), Quebec City, QC, Canada, 3–7 October 2012; pp. 23–27.

[22] Petrov S.V., Zhovtyansky V.A., Korzhyk V.N., “Technology and Equipment for Organic Waste Steam Plasma Processing”, International conference associations with solid waste (ISWA) “Advanced Recycling Technologies and waste disposal”, May 31- June 2, Moscow, 2011

4 Thermal gasification by VTT

Contributing author
Veli-Matti Pulkkanen, VTT

4.1 Gasification test facility and test procedure

Two bench-scale gasification test runs were carried out with unspent organic ion exchange resin (IXR), that was used already in the EU-THERAMIN-project few years ago [23]. The target was to produce treated material for further immobilisation and characterisation tests.

The gasification test trials were carried out with an atmospheric pressure bench-scale Bubbling Fluidised Bed (BFB) gasifier (Figure 34) at Bioruukki - VTT's Piloting Center (THERAMIN, 2019). The bed diameter of the reactor is 100 mm and the freeboard diameter 150 mm. The test facility is heated with external electrical heaters to compensate heat losses, and fluidising gases are preheated electrically to about 310°C below the grid.

The start-bed was added into the reactor as a batch before the fuel feeding was started. Al_2O_3 was used as a bed material. The IXR was fed from the live-bottom fuel tank equipped with the screw feeder. The gasification product gas was cleaned by a high-temperature filter unit. Easily volatile compounds condensate to the particles when the gas is cooled down to the temperature low enough and harmful compounds (e.g., Cs) are removed from the process with the filter dust.

IXR has such low ash content that bottom ash removal was not needed during the treatment process. No additional bed material was needed after the start-up. Minimised need for make-up bed material reduces the overall bottom ash waste, which has to be immobilised and disposed in a similar way as filter ash.

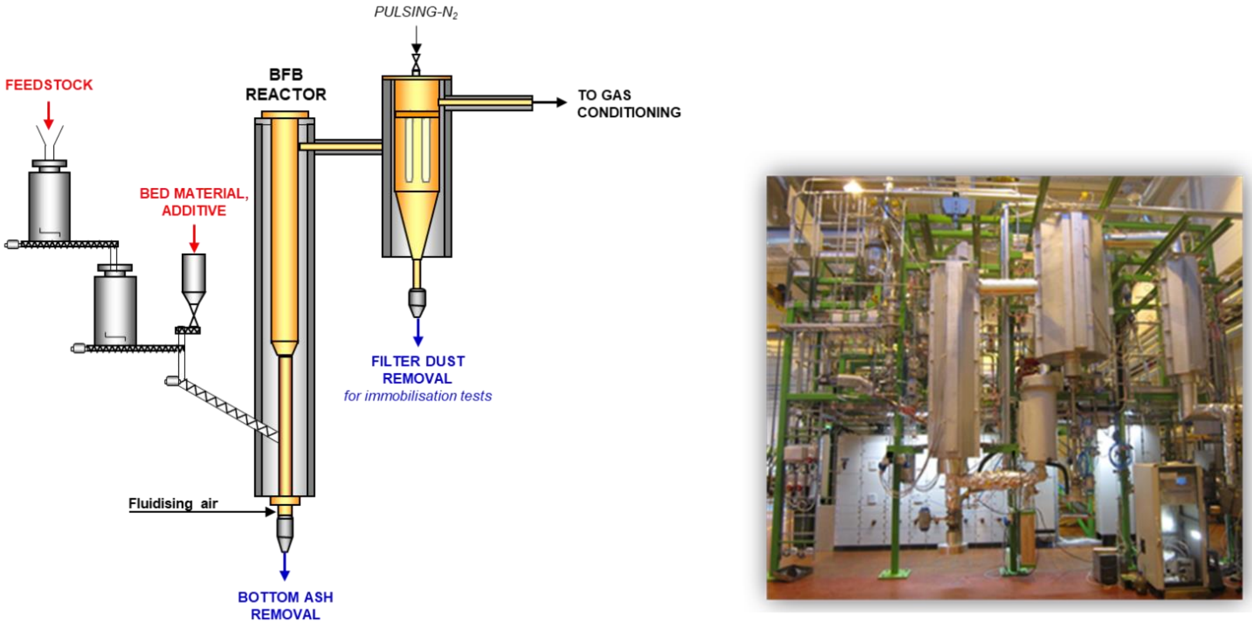

Figure 34. Bench-scale atmospheric-pressure gasification test rig (BFB100).

4.2 IXR feeds

At first IXR was impregnated with cesium, europium, and cerium in one batch, which was used in PR-3 test run. For the next test run PR-4, some iron was added to the IXR, which contained already those three other elements. The feeds are presented in Figure 35.

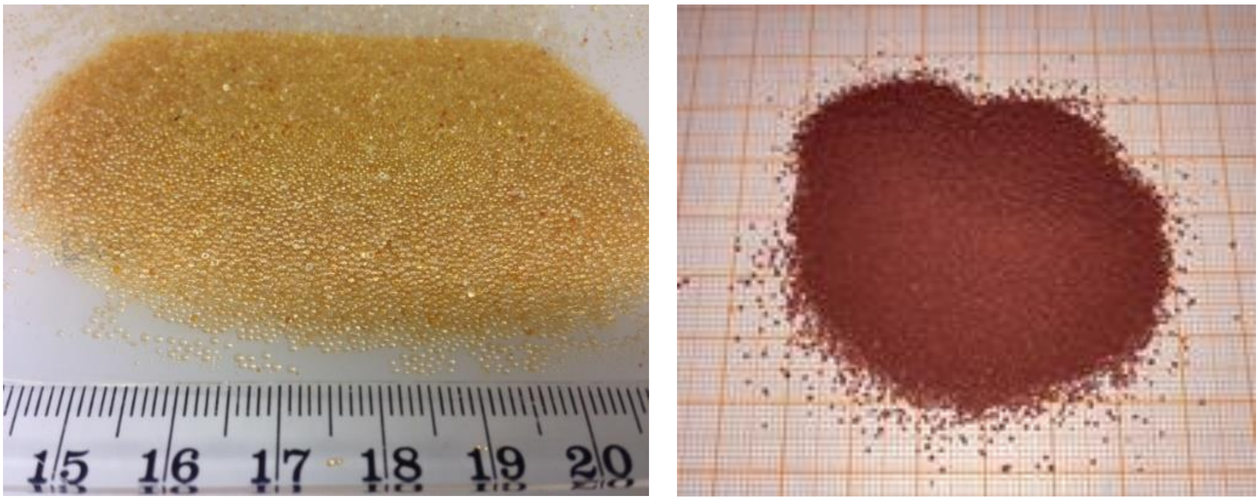

Figure 35. IXR for test run PR-3 (left) and for test run PR-4 (right).

4.3 Test run summaries

Summary of the test run PR-3 is in Table 10. Measured contents of the added elements in the feed were about 5 to 10 ppm. Iron was not added to the feed for this test run, but it was found, however, quite much in the filter dust. This was originated from the test facility, from its inner surface due to the corrosion and erosion. In addition, the test facility has a memory effect due to the fact, that some elements (e.g. Fe) are released later in the further test runs contaminating another samples. Therefore a specific cleaning run is needed before the actual test run when very low concentrations of a certain element are measured.

Table 10. PR3 test run summary.

Measured content, ppm-wt%	**Cs**	**Eu**	**Ce**	**Fe**
In dry feed	9.7	5.1	8.1	44
In filter dust	293	38	66	4380
• T(gasification) = 850-903ºC • T(filtering) = 406-426ºC • About 16.6 kg dry feed resulted in 680 g filter dust (during 25 hours)				

Gasification conditions in the test run PR-4 were quite similar to the previous run (Table 11). There was Fe addition to the feed for this test run, and the filter dust had high enough levels of all these elements for the further immobilisation tests.

Table 11. PR4 test run summary.

Measured content, ppm-wt%	Cs	Eu	Ce	Fe
In dry feed	9.9	8.9	8.5	28 500
In filter dust	250	73	114	373 400
• T(gasification) = 882-900ºC • T(filtering) = 406-423ºC • About 12.5 kg dry feed resulted in 630 g filter dust (during 16 hours)				

4.4 Chemical characterization

Concentrations of Al, As, Ca, Cd, Ce, Co, Cr, Cs, Cu, Eu, Fe, K, Mn, Mo, Na, Ni, P, Pb, S, Si, Sr, Ti, V, Zn, Ba in 11 solid samples (Table 12) were measured with ICP-OES (5100 SVDV, Agilent Technologies) and ICP-MS (Thermo Scientific Element 2),. The samples were taken during the steps of the gasification process (PRE1: only start bed, PRE2-3: dry feed pre-gasification IXRs, PRE4-5: material remaining in the bed of the BFB rig, PRE6: cleaning run, PRE7-8: dry feed pre-gasification IXRs with Fe_2O_3, PRE9-10: PR-3 and PR-4 test trials filter dusts, PRE11: cleaning run, and PRE12: control sample). The samples were digested with microwave equipment and diluted 1/50 to ICP-MS measurement and 1/2 to ICP-OES measurements. Representative background correction was performed, and dilution factors have been taken into account in the results. Multi-elemental standard solutions provided by Inorganic Ventures and SPEX were used as standards and control samples in the ICP-OES and HR ICP-MS measurement. NIST coal fly ash standard 1633b was used as a control sample for the digestion process. Uncertainty of the analysis is 10 %.

Table 12. Measured concentrations. Concentrations below the limit of detection are highlighted in light red and the sample specific limit of detection is stated.

Element/ isotope	Method	Sample / OES wavel. (nm)	PRE1 Al2O3	PRE2 Resin 1	PRE3 Resin 2	PRE4 BFB/PR-4 Remaining bed	PRE5 BFB/PR-4 Remaining bed	PRE6 BFB/PR Cleaning run	PRE7 Resin+ Fe2O3	PRE8 Resin+ Fe2O3	PRE9 BFB/PR-3 Filter dust	PRE10 BFB/PR-4 Filter dust	PRE11 BFB/PR-2 Cleaning run filter dust	PRE12 Coal Fly Ash
Al	OES	237,312	4677,47	<9,37	8,96	3730,81	4498,98	6446,67	15,51	<12,08	5044,84	4434,52	8268,81	52031,18
Ba-137	MS		1,52	<0,25	0,86	2,09	2,26	13,96	0,60	0,45	39,14	16,47	53,96	662,74
As-75	MS		<0,91	<0,83	<0,80	<1,04	<0,75	<0,98	<1,02	<1,03	22,92	12,10	15,59	134,07
Ca	OES	317,933	<207,19	<180,08	<176,65	<234,77	<168,87	1269,11	<231,28	<232,12	2958,85	1303,43	5741,39	15005,60
Cd-111	MS		<0,10	<0,09	0,12	<0,11	<0,08	<0,11	<0,11	<0,11	1,60	0,61	4,01	0,78
Ce-140	MS		<0,06	8,49	7,78	17,35	5,11	0,52	8,38	8,54	65,83	113,87	37,83	67,83
Co-59	MS		<0,67	<0,60	<0,58	2,95	1,55	4,66	<0,74	<0,75	5,93	19,02	49,97	46,47
Cr	OES	267,716	<4,39	<3,82	<3,75	361,08	124,13	243,96	15,15	11,60	1038,26	1249,48	4779,90	206,18
Cr-52	MS		<3,45	<3,12	<3,01	323,72	108,92	218,95	14,32	9,45	966,22	1140,68	4547,71	184,28
Cs-133	MS		<0,06	9,75	9,66	1,32	1,53	0,08	8,82	10,99	292,87	250,37	103,74	8,37
Cu	OES	217,895	<13,88	<12,06	<11,83	38,71	31,39	<14,97	<15,49	<15,55	175,48	148,41	348,18	139,78
Cu-63	MS		2,62	<1,76	2,28	34,88	20,01	12,15	<2,17	<2,18	171,77	133,91	321,50	109,20
Eu-153	MS		<0,07	5,60	4,66	13,00	5,37	0,45	7,77	9,96	37,98	73,38	22,89	0,75
Fe	OES	239,563	43,22	<5,83	33,42	3021,33	10568,38	5514,49	31766,96	27573,29	4527,28	363803,01	350093,89	66943,19
Fe-56	MS		<59,61	<54,05	<52,04	2819,46	9582,94	5101,59	28955,70	25775,47	4224,87	382955,04	366441,76	60813,15
K	OES	769,897	<3,82	<3,32	<3,26	<4,33	<3,11	<4,12	<4,26	<4,28	<4,43	<4,41	291,93	5637,08
Mn	OES	261,02	<4,16	14,42	<3,55	<4,72	<3,39	83,54	<4,65	8,21	17,64	678,34	1161,32	67,45
Mo	OES	268,799	<11,45	<9,95	<9,76	<12,98	9,19	<12,34	<12,78	<12,83	39,20	175,50	369,10	1154,55
Na	OES	589,592	217,52	<4,82	6,87	100,41	151,02	234,70	8,99	9,03	308,02	232,76	613,06	997,71
Ni-60	MS		<4,20	<3,81	<3,67	1309,60	392,26	577,74	<4,70	<4,72	940,60	2626,43	7369,38	121,75
P	OES	177,434	<79,95	<69,49	<68,16	<90,59	<65,16	<86,26	<89,24	<89,57	<92,63	<92,39	<72,01	2375,95
Pb-208	MS		0,19	0,09	0,31	0,03	0,07	0,09	0,15	0,13	61,38	40,04	125,03	72,52
S	OES	181,972	<89,09	70589,27	70629,24	1146,55	165,66	124,48	66813,26	70179,98	48331,04	118026,88	16428,15	2189,88
S-32	MS		<101,40	75017,11	68436,12	1131,99	194,70	<109,32	65891,85	67983,98	48641,95	114700,37	15694,21	1939,36
Si	OES	221,667	1383,89	1184,34	1660,39	941,07	1187,72	155,77	<36,42	502,36	1713,33	1010,07	3170,32	220426,91
Sr-88	MS		0,60	0,11	0,46	0,48	0,49	6,12	0,52	0,06	6,80	3,10	19,50	960,21
Ti	OES	337,28	<0,51	<0,45	<0,44	3,06	1,54	0,30	0,76	<0,57	154,80	50,32	68,85	7771,73
V-51	MS		<0,55	<0,50	<0,48	<0,62	<0,45	<0,59	<0,61	<0,61	3,57	11,04	20,38	276,89
Zn-66	MS		6,60	1,20	2,36	40,37	16,90	22,96	<0,98	<0,99	585,49	300,24	1466,83	221,24
Unit			mg/kg	mg/kg	mg/kg	mg/kg	mg/kg	mg/kg	mg/kg	mg/kg	mg/kg	mg/kg	mg/kg	mg/kg

4.5 Conclusions

VTT's thermal gasification process was successfully used to produce enough amounts of thermal treated waste for further testing in Tasks 6.4 and 6.6. The process was verified to be a suitable thermal treatment method for organic IXR in EU-THERAMIN-project.

REFERENCES

[23] THERAMIN. 2019. Thermal treatment for radioactive waste minimisation and hazard reduction. D3.4 of THERAMIN project in EU's Horizon 2020 programme.

5 Thermal incineration of solid organics and SIERs surrogates by CEA

Contributing author
Hélène Nonnet, CEA

5.1 Description of the incineration process

The ashes considered in these studies come from the IRIS incineration pilot process (Installation for Research on Incineration of Solids) developed at CEA Marcoule for R&D support and devoted to the treatment of the organic waste contaminated by α-emitting actinides from glove boxes in the nuclear industry.

This pilot is working exclusively under inactive environment, and the ashes produced come from the incineration of a mix of different organic solids and IER resins. This leads to achieve a volume reduction of the waste to about a 30 factor. IRIS is a three-step process implemented in rotating kilns.

The first step consists in oxidative pyrolysis at 550°C, producing pitch that is then processed in a calcining step at 900°C in oxygen-enriched atmosphere. The off-gases arising from the thermal treatments include a volatile hydrocarbon fraction that is oxidized at 1100°C in an afterburner.

This multistep process has two advantages. The elimination of chlorine at low temperature in the pyrolyzer limits corrosion problems and allows operation with low gas flow, which also limits particle entrainment. Adding oxygen during the pyrolysis step oxidizes the heavy hydrocarbons that produce tars capable of forming deposits in the ducts. Forming during the pyrolysis step, the pitch drops into the calciner being a rotary kiln heated at 900°C. The pitch remains around 2 hours in this furnace and is transformed into ashes having a very low carbon content (< 1%). Before discharge to atmosphere, the gas stream is submitted to caustic scrubbing to eliminate the volatile acids.

The material balance in the process is about as follow: a feeding rate of 4kg/h produces around 1550g/h of pitch, 111 g/h of ashes and 47g/h of dust.

Although this technology limits corrosion, it does not completely prevent the production of metal chlorides [24].

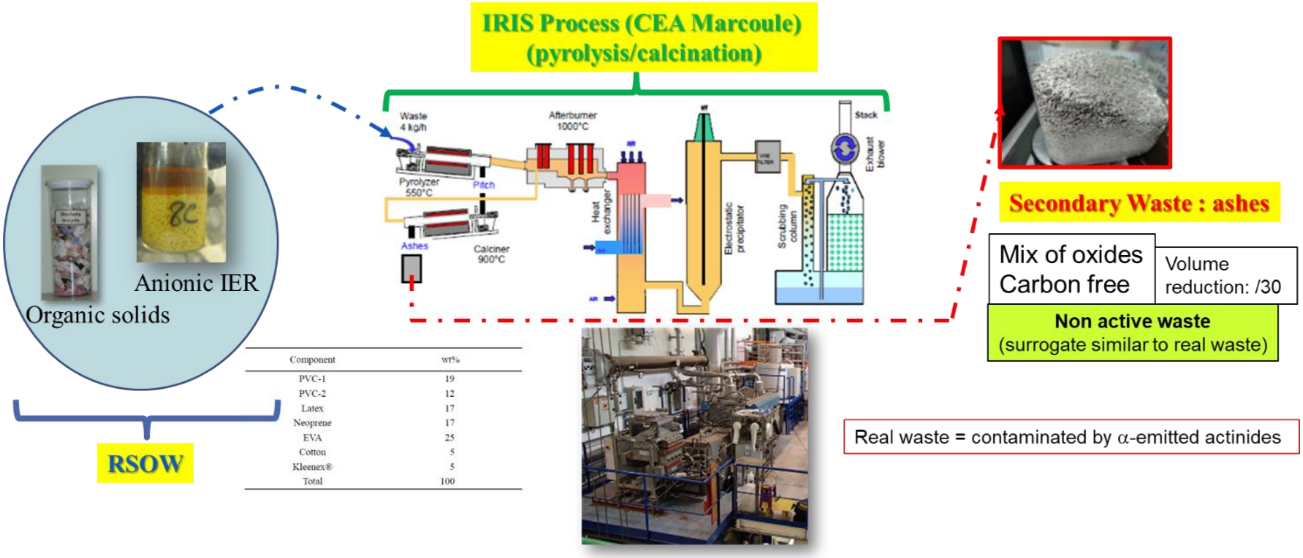

Component	wt%
PVC-1	19
PVC-2	12
Latex	17
Neoprene	17
EVA	25
Cotton	5
Kleenex®	5
Total	100

5.2 Characterization of the ashes

The ashes have a high flying behaviour with a density of 0.2 $g.cm^{-3}$ and their particle size is mainly centered between 0.1 to 1 mm (Figure 36).

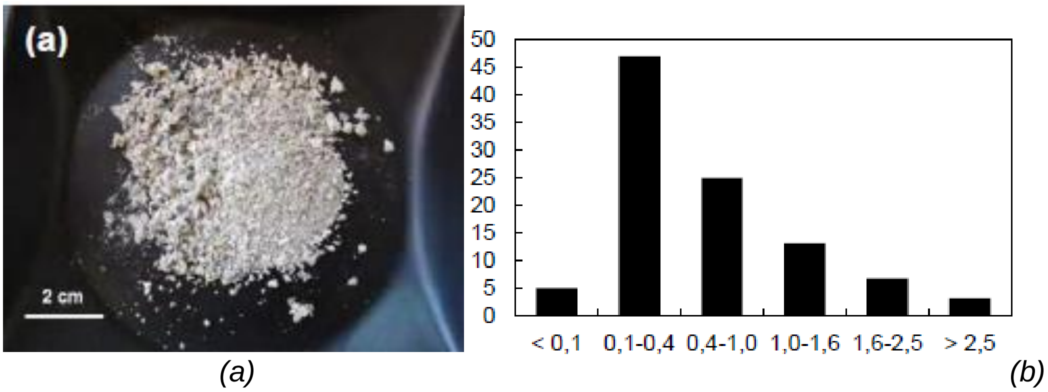

(a) *(b)*

Figure 36. (a) IRIS ashes general morphology, (b) IRIS ashes granulometric class.

5.2.1 Elementary analysis

Elementary chemical characterisations have been done. The ashes are mainly composed of aluminium, silicon, calcium and zinc Table 13.

Table 13 Chemical analysis of the IRIS ashes.

Component	%weight
C	0,20
Cl	1,74
S	0,57
Ba	0,13
Cr	0,06
Al	15,06
Fe	0,44
Mg	2,73
K	3,00
Ti	0,41
P	1,83
Na	0,70
Ca	9,68
Si	13,72
Ni	0,48
Zn	5,76
Bi	0,11
Σ	56,63
O (difference)	43,367
	100,00

Component	%weight
Cl	1,81
SO3	1,47
BaO	0,15
Cr2O3	0,09
Al2O3	29,55
Fe2O3	0,65
MgO	4,70
K2O	3,73
TiO2	0,72
P2O5	3,36
Na2O	0,99
CaO	14,07
SiO2	30,48
NiO	0,64
ZnO	7,45
Bi2O3	0,13
	100,00

5.2.2 SEM analysis of the ashes

SEM and structural characterizations have been done. The micro particles have a very porous aspect and are partially amorphous. The crystallized phase are composed of ringwoodite, anohrtite and chlorapatite $Ca_5(PO_4)_3Cl$

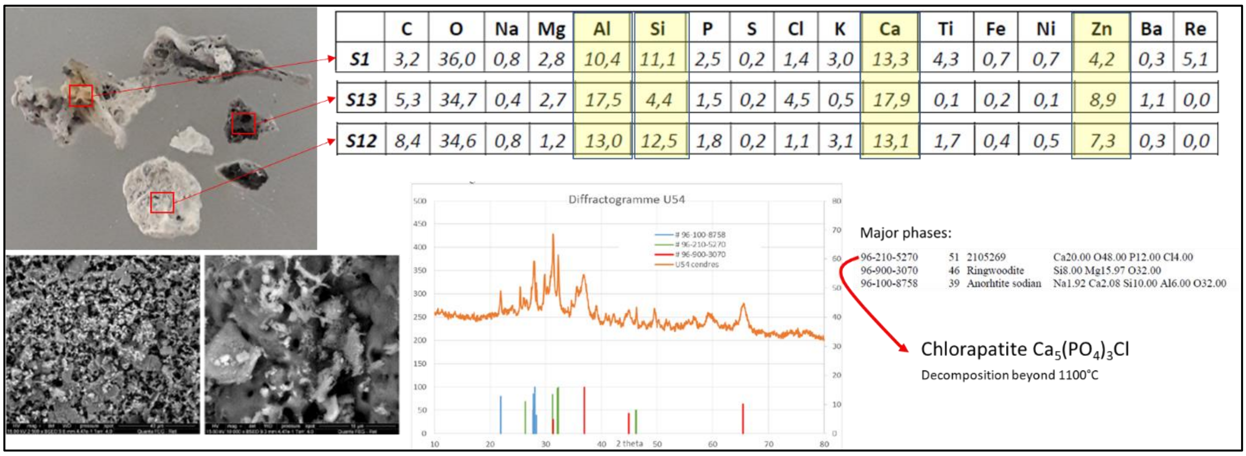

	C	O	Na	Mg	Al	Si	P	S	Cl	K	Ca	Ti	Fe	Ni	Zn	Ba	Re
S1	*3,2*	*36,0*	*0,8*	*2,8*	*10,4*	*11,1*	*2,5*	*0,2*	*1,4*	*3,0*	*13,3*	*4,3*	*0,7*	*0,7*	*4,2*	*0,3*	*5,1*
S13	*5,3*	*34,7*	*0,4*	*2,7*	*17,5*	*4,4*	*1,5*	*0,2*	*4,5*	*0,5*	*17,9*	*0,1*	*0,2*	*0,1*	*8,9*	*1,1*	*0,0*
S12	*8,4*	*34,6*	*0,8*	*1,2*	*13,0*	*12,5*	*1,8*	*0,2*	*1,1*	*3,1*	*13,1*	*1,7*	*0,4*	*0,5*	*7,3*	*0,3*	*0,0*

Major phases:

96-210-5270	51	2105269	Ca20.00 O48.00 P12.00 Cl4.00
96-900-3070	46	Ringwoodite	Si8.00 Mg15.97 O32.00
96-100-8758	39	Anorhtite sodian	Na1.92 Ca2.08 Si10.00 Al6.00 O32.00

Chlorapatite $Ca_5(PO_4)_3Cl$

Decomposition beyond 1100°C

Figure 37. *SEM and XRD characterizations of the IRIS ashes.*

REFERENCES

[24] Lemont F. Management of metal chlorides in high temperature processes--application to the nuclear wastes treatment. J Hazard Mater. 2012 Apr 30;213-214:38-45.doi: 10.1016/j.jhazmat.2012.01.038. Epub 2012 Feb 3. PMID: 22365141.

6 Plasma vitrification developed at USFD

Contributing authors
Josh Radford, Claire Corkhill, USFD

The use of Plasma vitrification for the treatment of nuclear waste has been assessed, showing that vitrified waste products can be successfully produced with less requirement for waste pre-treatment compared to other thermal treatments. A case study has demonstrated the viability of plasma vitrification and the chemical and physical properties of the pre-treated waste and the final wasteform are presented here.

6.1 Plasma Vitrification

6.1.1 Plasma Vitrification Capabilities

Plasma vitrification has been demonstrated as a potential treatment method for a range of hazardous and radiological wastes. In comparison to other thermal treatment options (HIP, conventional vitrification/melting), plasma vitrification can offer similar advantageous wasteform characteristics such as a high chemical durability, high density and good volume reduction whilst also being versatile when considering waste input properties. Due to the high temperatures employed during the plasma vitrification process, pre-treatment of wastestreams can be minimised in comparison to other thermal treatments whilst still producing wasteforms that can meet Waste Acceptance Criteria.

Conventional vitrification systems are generally limited to processing temperatures of < 2000°C, whereas in theory, plasma vitrification is capable of reaching temperatures of up to 20000°C, with typical processing temperatures around 3000°C [25]. The high processing temperatures employed in plasma vitrification allow for minimal waste pre-treatment, with several successful studies demonstrating waste in steel waste drums being vitrified directly. With careful wasteform design, it is possible process wastestreams with large variations in composition to produce glassy wasteforms with acceptable wasteform characteristics.

6.1.2 Case Study of Plasma Vitrified Wasteforms

6.1.2.1 Introduction

Simulant Plutonium Contaminated Material (PCM) was processed using plasma vitrification by Tetronics Ltd in the UK [26-28]. Characterisation of the resultant wasteform was undertaken at the University of Sheffield (USFD) and presented here [29]. The simulant wastestream was representative of the 200 L steel drums containing PCM at the Sellafield site in the UK. Several variants of PCM were considered to represent the different contaminated materials (wood and organics, masonry and construction materials, PVC from packaging and handling), several 100 L steel drums were prepared with the different PCM waste streams and directly vitrified with suitable glass forming additives (GFA) to produce a stable, durable wasteform. The GFA chosen for this study was a calcium aluminosilicate slag, with the aim of producing a wasteform based around the Anorthite/Pseudowollastonite composition. For all trials conducted by Tetronics Ltd, the composition of the wastestreams had little influence on the final wasteform composition due to the limited amount of inorganic materials present. Trial 1 contains a large amount of building materials (see Table 14) and therefore required less GFA to produce a wasteform within the required compositional envelope. Trial 5 contains a large amount of organic material and therefore required operational adjustments to ensure full oxidation of the organic components and prevent localised overheating. Full oxidation of these components was accomplished by injecting a combination of water and air to the system at a rate of 5 L/h and 27 m^3/h respectively. For both trials discussed here an initial 5 kg of GFA was initially introduced to the crucible with the respective 100 L waste drum (i.e. whilst the crucible was cold).

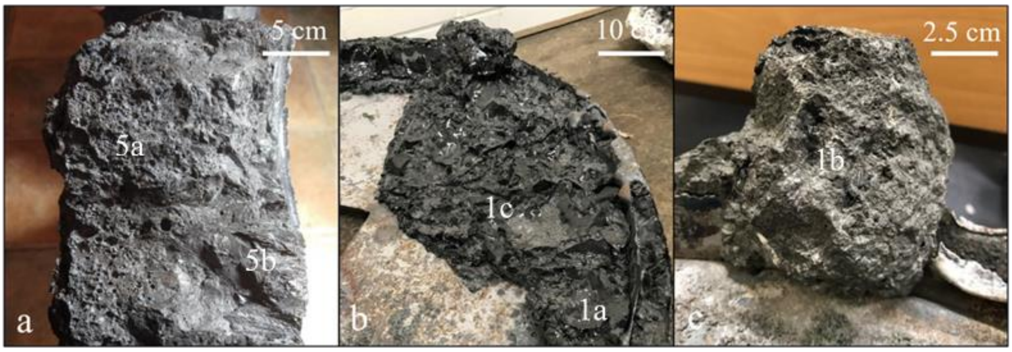

Figure 38. Example images of the vitrified PCM wasteforms. a) Material from Trial 5, b) Trial one, Sample 1a and 1c, c) Trial 1, Sample 1b.

When this initial material formed a melt pool, additional GFA were fed into the furnace, with the amount required depending on the wastestream composition.

6.1.2.2 Analysis of the resultant wasteform

The composition of the pre-treated waste can be seen in Table 14Table 13, these compositions are representative of the range of materials found in PCM wastestreams. Several samples were selected for analysis and were characterised by XRD, SEM-EDX and XRF. All samples related to trial 1 and trial 5 of the Tetronics study. Three regions of interest were identified from trial 1, a glassy sample (Sample 1a) and two glass-ceramic samples (Sample 1B and Sample 1C). All samples from trial 1 share similar chemistry (see Table 15) but vary in their degree of crystallinity. Two more samples were selected from trial 5, Sample 5a represents a dense crystalline phase taken from the edge region of the wasteform (i.e. closer to the crucible wall) and Sample 5b represents a porous region from the centre of the wasteform.

Figure 39 shows the XRD patterns for all samples analysed. The main crystalline phase observed is Anorthite ($CaAl_2Si_2O_8$), which was expected given the area of the CaO-Al_2O_3-SiO_2 phase diagram that Tetronics where targeting for the final wasteform compositions. Samples from trial 5 also show evidence of an Fe_2O_3 crystalline phase, most likely from the oxidation of the metallic drum material. The formation of the crystalline phases could be suppressed either by compositional modification of the GFA or by modifying the operational process to ensure a faster cooling regime. However, these options may be unnecessary as the crystalline phase formed is highly durable and does not adversely affect any desirable wasteform properties.

Table 14. Simulant PCM Drum Compositions [27].

Constituent	Trial 1	Trial 2	Trial 3	Trial 4	Trial 5
Container	17.4	17.42	17.36	17.4	17.4
PVC Liner	1.52	1.52	1.86	1.52	1.52
Steel Drum Liner	8.74	8.82		8.78	8.84
Bricks	18.04				
Concrete	17.14				
Mild Steel Pipe		5.58			
Galvanised Sheet Steel		1.30			
Cast Iron		2.00			
Stainless Steel Pipe		1.06			
1 Beam		10.26			
Steel Scaffolding		9.84			
Aluminium Scaffolding		0.98			
Steel Plate		5.20			
Copper Pipe		0.28			
Hand Tools and Equipment			20.16		
Rubber Hose			1.78		
Wellingtons			1.86		
PVC Suits and Storage Bags			7.24		
Paper			0.13		
Scaffolding Board			1.88		29.4
Lab Glassware			0.56		
Floor Sweepings			0.54		
Vermiculate and Water			0.25		
Strippable Coating (Decongelsure)			0.32		
Polybottles			0.27		
Alumina Furnace Bricks			0.57		
Electrical Cabling			0.55		
Rubber Gloves			0.25		
PVC Suits			12.9		
Total	62.84	64.29	55.57	40.60	57.16

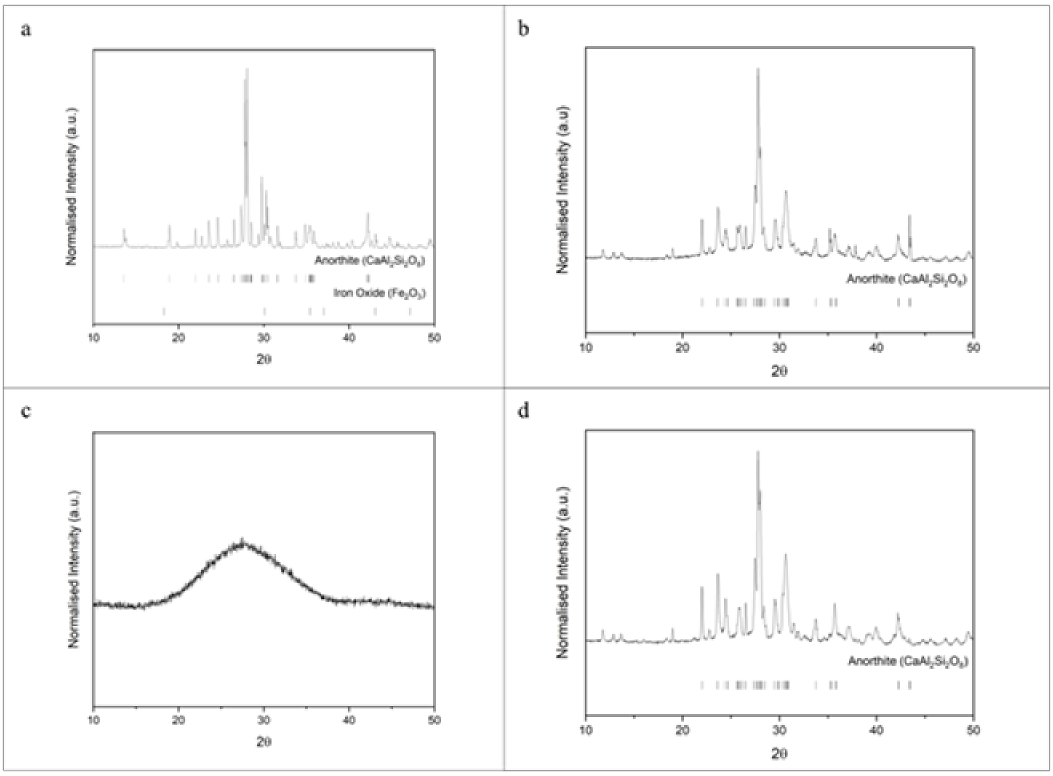

Figure 39. XRD patterns for samples: a) Sample 5a (also representative of Sample 5b), b) Sample 1b, c) Sample 1a, d) Sample 1c.

Figure 40 shows a low magnification of a sample from Trial 1, with regions representative of Samples 1a, 1b and 1c (the glassy and crystalline components).

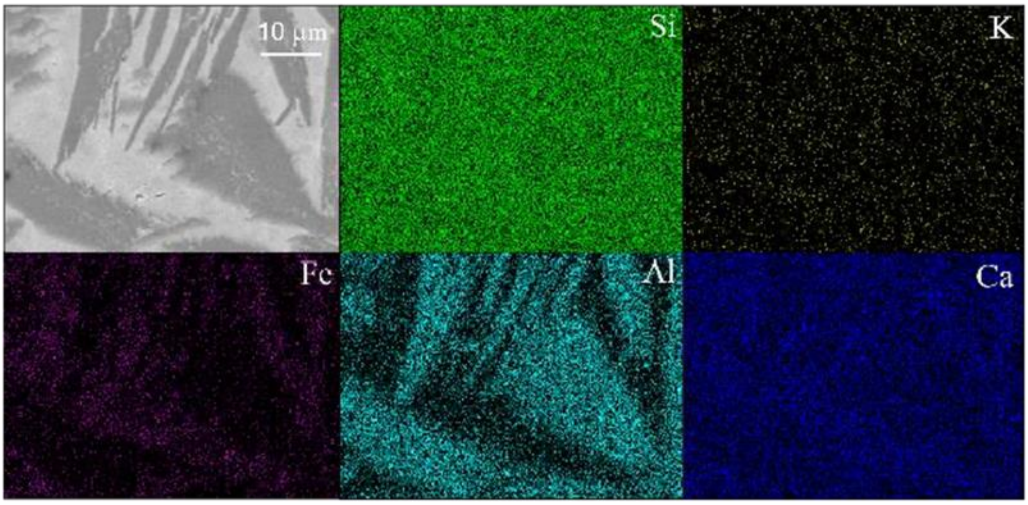

Figure 41 shows a higher magnification SEM image and the corresponding EDX maps representative of samples 1b and 1c. Two distinct phases can be observed in Figure 41, the lighter region is Fe rich, whilst the darker region, rich in Ca, Al and Si is attributed to the Anorthite phase, in agreement with the XRD analysis.

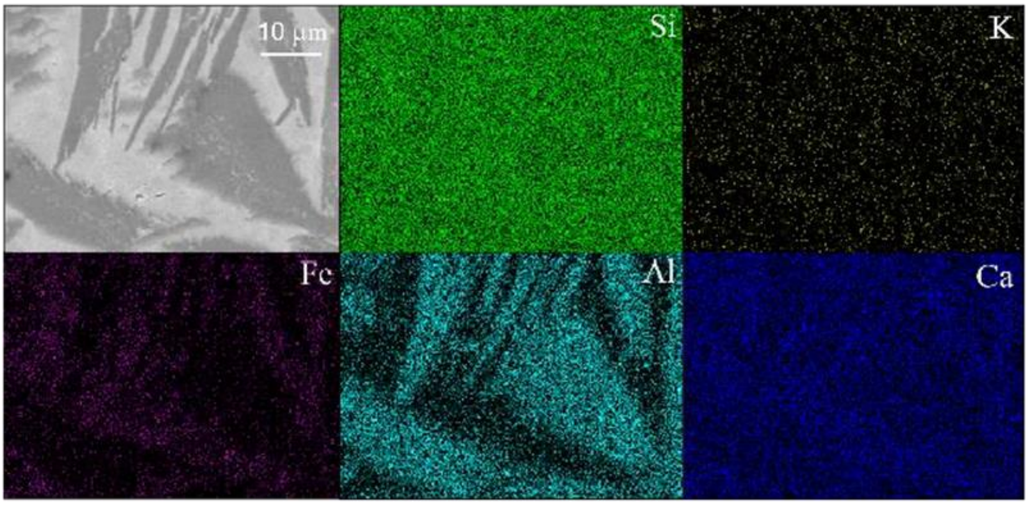

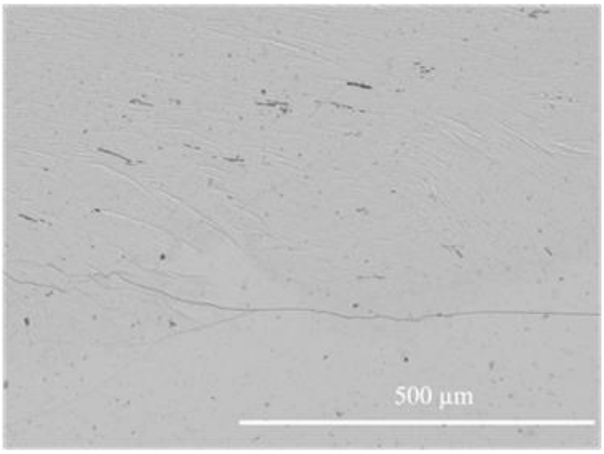

Figure 40. SEM image of a sample from trial 1 with the different areas of interest labelled (a - glassy region, sample 1a; b – crystalline region, sample 1b and 1c.

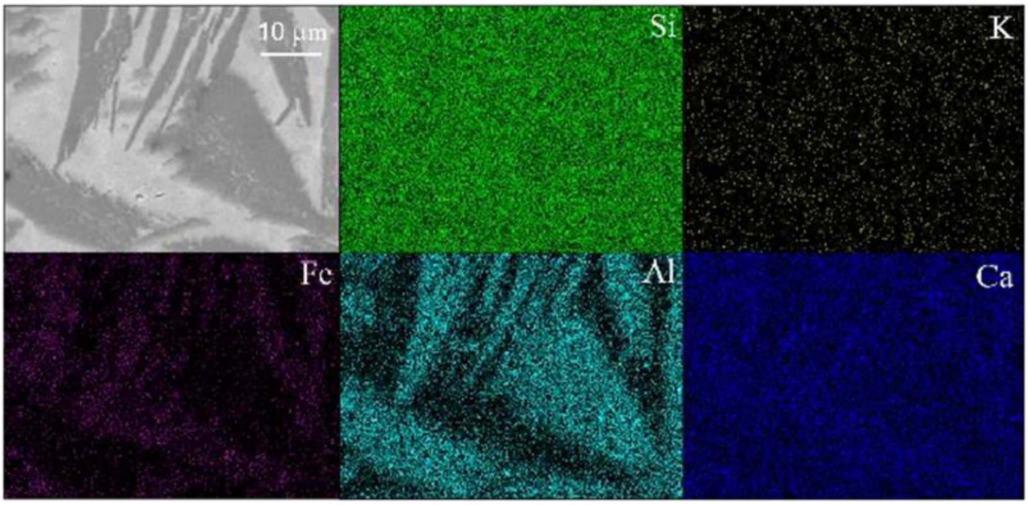

Figure 41: SEM image and EDX maps for sample representative of Sample 1b and 1c.

Figure 42 compares the porosity of Samples 5a and 5b, with Figure 42a having large pore regions within a similar crystalline microstructure to that of Figure 42b. This is in agreement with the XRD analysis shown in Figure 39 that the dominant crystalline phase found in these samples is Anorthite. Figure 42 shows the EDX maps for Sample 5a, highlighting an Fe rich inclusion, most likely responsible for the Fe_2O_3 identified in the XRD analysis

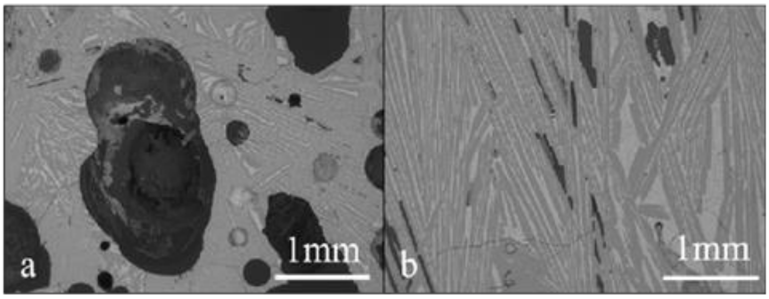

Figure 42: Comparison of Sample 5a (right) and Sample 5b (left)

The chemical composition of all samples was confirmed using XRF spectroscopy and the analysed compositions of each sample can be seen in Table 15. All compositions are in good agreement with the target compositional envelope identified by Tetronics Ltd in this study.

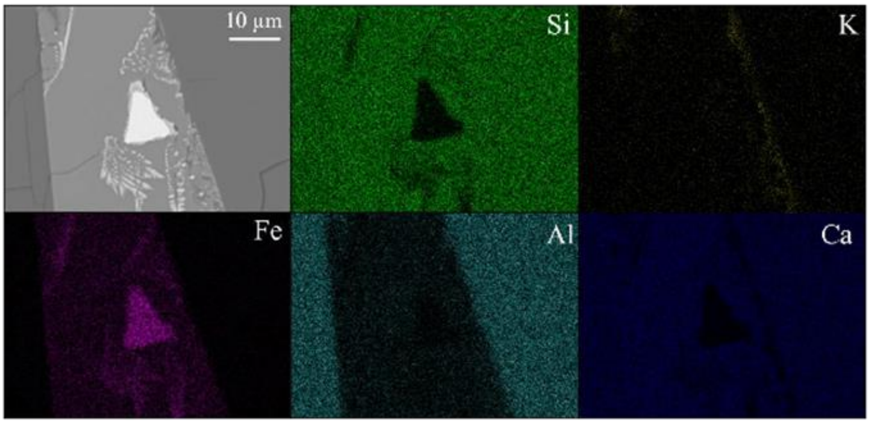

Figure 43: SEM image of sample 5a and corresponding EDX maps.

Table 15. Analysed Composition of Selected Samples (wt.%).

Oxide	Sample 5a	Sample 5b	Sample 1a	Sample 1b	Sample 1c
SiO_2	46.05	47.91	54.92	54.66	53.87
Al_2O_3	19.73	18.86	13.21	13.72	14.56
B_2O_3	0.18	0.24	0.30	0.12	0.13
BaO	0.03	0.03	0.04	0.04	0.04
CaO	17.07	16.12	18.71	18.49	18.98
Cr_2O_3	0.11	0.11	0.07	0.11	0.06
Fe_2O_3	14.62	14.61	10.20	10.41	9.78
K_2O	1.00	0.92	1.08	0.97	1.11
MgO	0.18	0.147	0.58	0.56	0.59
MnO_2	0.08	0.08	0.06	0.06	0.06
Na_2O	0.07	0.07	017	0.17	0.18
P_2O_5	0.35	0.33	0.36	0.39	0.33
SrO	0.02	0.02	0.02	0.02	0.02
TiO_2	0.48	0.47	0.23	0.23	0.25
ZnO	0.04	0.03	0.05	0.05	0.05
ZrO_2	0.01	0.01			

6.2 Conclusions

Plasma vitrification has been demonstrated to be a possible immobilisation route for several wastestreams. The key benefit to using plasma vitrification over other thermal treatments is the minimal pre-treatment of wastes prior to the vitrification process as the study discussed here demonstrates the capability of processing wastestreams directly from storage drums. In addition to the lack of pre-treatment required, plasma vitrification is capable of producing durable and stable wasteforms comparable to those produced using alternative thermal processing routes. The samples discussed in this report represent the variation in chemical composition found in PCM wastes in the UK. Despite the difference in the composition of the wastestream, all wasteforms were successfully produced to be within the target compositional envelope, demonstrating the operational flexibility of plasma vitrification.

REFERENCES

[25] E. Gomez, D. A. Rani, C. R. Cheeseman, D. Deegan, M. Wise, and A. R. Boccaccini, 'Thermal plasma technology for the treatment of wastes: A critical review', J. Hazard. Mater., vol. 161, no. 2–3, pp. 614–626, Jan. 2009, doi: 10.1016/j.jhazmat.2008.04.017.

[26] Tetronics International, ‘Nuclear Plasma Trials: Drum Preparation.pdf’, 1107-01-TD001-R01, 2019.
[27] Tetronics International, ‘CONSTAIN Plasma Trials Procedure for Nuclear Demonstration Furnace’, 1107-02-TD001, 2019.
[28] Tetronics International, ‘Plasma PCM Trials Report for Nuclear Demonstration Furnace’, 1107-10-TD001-R01, 2020.
[29] D. Parkes, C. L. Corkhill, C. L. Thorpe, M. T. Harrison, and S. Morgan, ‘Analysis of Simulant UK PCM Waste Trials’, presented at the Waste Management Symposium, Phoenix, Mar. 2022.

7 Molten Salt Oxidation (MSO) thermal treatment process developed at CVRez

Contributing authors
Vojtěch Galek, Anna Sears, Petr Pražák, Martin Vacek, Jak Hadrava, CVRez

7.1 Introduction

The CVRez's main contribution to this report was using their Molten Salt Oxidation (MSO) thermal treatment process. During this process, waste is generated, which needs to be reprocessed or disposed of. This report shows the MSO process and characterises the generated waste. The possible disposal methods for this waste are described in Deliverable 6.2.

7.2 MSO process

MSO is a thermal process designed for the disposal of organic waste. Technology has been well-known since the end of the fifties of last century. This process is based on the flameless decomposition of organic wastes in high molten salt temperatures. Dosing an oxidising medium with the waste below the molten salt's surface is necessary to complete the organic material's oxidation [30]. Other non-combustible inorganic substances, i.e., heavy metals or possibly radionuclides, are trapped in the molten salt and can be easily separated. [30-33] All organic carbon-containing wastes, together with excess combustion air, are conducted in the reaction vessel below the level of the salt melt, which has a temperature of 800 – 950°C. The melt is usually Na_2CO_3, K_2CO_3, Li_2CO_3, or their eutectic mixtures.

The MSO process has several advantages over combustion. The operating temperature depends on the used alkali salts, but it is generally lower than in direct combustion. Alkaline carbonates and mixtures have melting temperatures from 400°C to 850°C. The alkaline molten salt also acts as a scrubber for other acidic substances such as SO_3, SO_4, and NO_x, eliminating the need for a flue gas cleaning system. The oxidation and neutralisation are shown in chemical equations (1 - 3). The molten salt has the function of a stable heat transfer medium which resists thermal shocks and is thus able to maintain rapid process fluctuations. This technology is also suitable for disposing of explosive materials, detonators, or other energetic materials [31,33-35].

Oxidation process:

$$2C_aH_b + (2a + \frac{b}{2})O_2 = 2aCO_2 + bH_2O \tag{1}$$

Nitrogen-containing wastes:

$$C_aH_bN_c + \left(a + \frac{b}{4}\right)O_2 = aCO_2 + \frac{b}{2}H_2O + \frac{c}{2}N_2 \tag{2}$$

Wastes containing halogens (X):

$$C_aH_bX_c + \frac{c}{2}Na_2CO_3 + \left(a + \frac{(b-c)}{4}\right)O_2 = \left(a + \frac{c}{2}\right)CO_2 + \frac{b}{2}H_2O + cNaX \tag{3}$$

Despite many advantages, MSO technology has its drawbacks. One of the main disadvantages is the increased economic cost when compared to combustion processes. It is necessary to heat the alkali salt to its melting point and keep it in a liquid state. After the initial heating, onward heating is ensured by the supply of waste and oxidising medium during the disposal of energy-rich wastes. Another disadvantage is the high corrosivity of the environment. Construction materials do not have a long service life if they are in contact with molten salts at high temperatures and in an oxidising environment [36,37].

In Figure 44, the MSO technology in CVRez is shown. It consists of two reactors and operates in the temperature range from 400 to 950°C. The temperature control in the reactors is separate and allows setting different temperatures in each reactor. The role of the second stage is often variable but basically complements the first one and is mainly used for the high-temperature oxidation of flue gases with a high carbon monoxide content, hydrocarbon residues and the capture of fly ash containing radionuclides. To achieve optimal oxidation, the temperature must be above 800°C, and it is preferable to operate the reactor at least 900°C to reduce the necessary residence time of the reactants in the reactor.

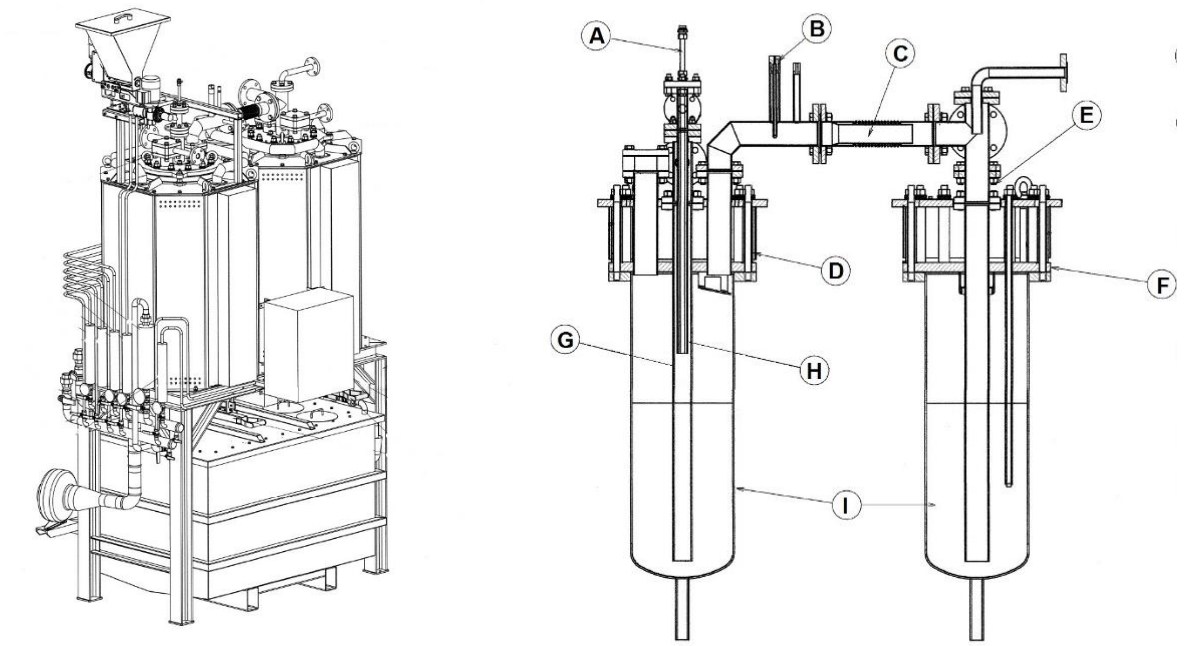

Figure 44. The detailed picture of the MSO reactors with the waste tank (left), the two reactor vessels connected in the two-stage system reactor system (right).

As the neutralisation and saturation of the salt take place during the experiment, salt discharge is needed. The spent salt is discharged via the “cold plug” at the bottom of the reactor vessel into the water tank. The cold plug is formed during the melting of the salt before the experiment starts. After the experiment, the dosing of the waste is stopped, and the bottom of the reactor is heated by induction, heating up to the melting point temperature. When the “cold plug” is melted, the molten salt is poured into the water tank and partially dissolved. The dissolved salt is drained, and the rest is manually taken and reprocessed into MSO waste, ready to be immobilised.

7.3 MSO waste

As the main generator of RSOW from the thermal treatment process of Molten Salt Oxidation CVRez was able to supply this waste to other partners. This waste must be removed from the storage tank and reconditioned for encapsulation. That means waste was pre-dried in the air, ground for smoother particles, and dried in the oven for 65°C to get low moisture levels as the moisture could negatively affect the final product. Figure 45 shows the XRD analysis of the dried-up waste salt samples.

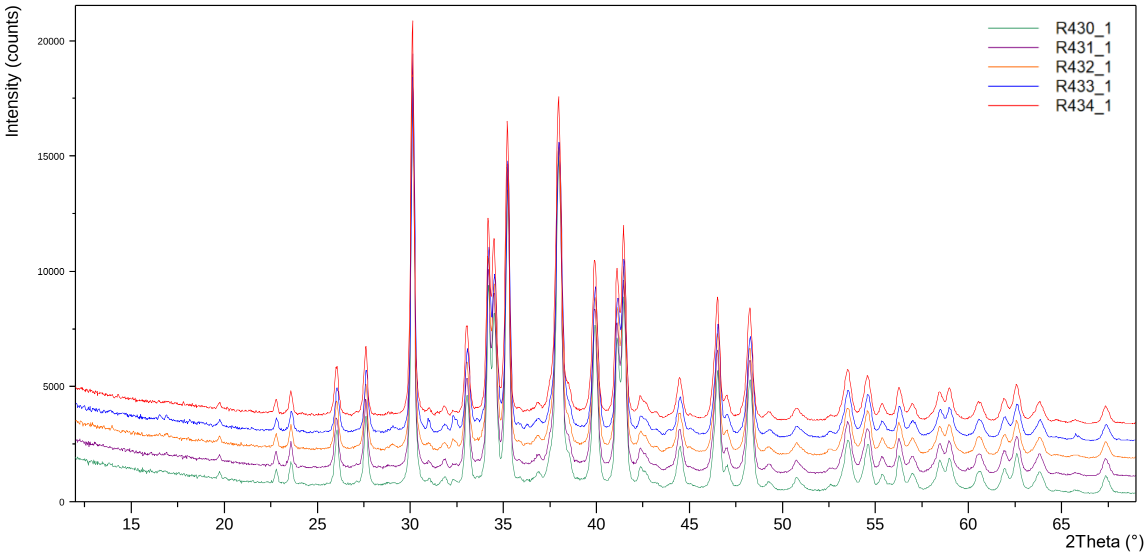

Figure 45. The XRD analysis of MSO waste salt samples.

Table 16 shows the weight % of the phase distributions in each sample with Natrite as the primary phase. The results show homogenous compositions throughout the bulk of the waste.

Table 16. The phase composition generated from XRD analysis of each sample by (w.%).

Phase		**R430**	**R431**	**R432**	**R433**	**R434**
Natrite	Na_2CO_3	96.41	96.52	95.07	94.12	96.25
Essenite	$CaFeAlSiO_6$	3.38	3.48	3.32	3.14	3.71
Thermonatrite	$Na_2CO_3{\cdot}H_2O$	0.21	-	0.79	1.79	0.04
Trona	$Na_3H(CO_3)_2{\cdot}\ 2H_2O$	-	-	0.81	0.95	-

The waste was very hygroscopic and contained Cs^+, Co^{2+} and Sr^{2+} tracers from thermally treated Ion Exchange Resins (IER).

The semiquantitative analysis of the MSO waste was also performed, and its results are shown in Table 17. The results are shown in weight % from each sample and show a minor constitution, but it can be assumed as background.

Table 17. The semiquantitative analysis of waste salt determined by w. %.

Ident		**R430**	**R431**	**R432**	**R433**	**R434**
Al_2O_3	*(%)*	7.48	6.23	7.29	3.8	6.38
CaO	*(%)*	0.137	0.161	0.142	0.134	0.148
Cl^-	*(%)*	0.066	0.072	0.064	0.073	0.076
Co_3O_4	*(%)*	0.029	0.038	0.031	0.026	0.036
Cr_2O_3	*(%)*	0.079	0.082	0.077	0.094	0.073
CuO	*(%)*	0.009	0.007			
Fe_2O_3	*(%)*	0.26	0.19	0.22	0.22	0.24
K_2O	*(%)*	1.647	1.67	1.663	1.744	1.585
MgO	*(%)*	0.223	0.269	0.255	0.261	0.252
MnO	*(%)*		0.01			
Na_2O	*(%)*	81.927	84.662	82.448	89.283	84.185
NiO	*(%)*	0.243	0.219	0.233	0.246	0.222
P_2O_5	*(%)*	0.009	0.009	0.013	0.009	0.01
SO_3	*(%)*	0.164	0.263	0.176	0.193	0.157
SeO_2	*(%)*		0.003			
SiO_2	*(%)*	7.494	5.959	7.193	3.763	6.434
SrO	*(%)*	0.034	0.034	0.034	0.035	0.031
TiO_2	*(%)*	0.15	0.082	0.12	0.077	0.13
ZnO	*(%)*	0.043	0.041	0.04	0.041	0.045

The humidity of the samples was also determined because this could affect the mechanical properties of the prepared geopolymer samples. As the Na_2CO_3 and its hydrates are highly hygroscopic, the blooming effect and swelling take place, which causes cracks in the samples, which leads to stability loss [38].
Table 18. The moisture content in the measured samples (w.%)Table 18 shows the humidity of the analysed samples. Different compositions with Trona and Thermonatrite present can determine the changes in the sample R432.

Table 18. The moisture content in the measured samples (w.%).

Moisture	**R430**	**R431**	**R432**	**R433**	**R434**
Weight %	1.31	1.31	4.20	1.48	1.20

This MSO salt waste samples were delivered to other partners to study their immobilisation techniques and options. Samples were delivered to SCK CEN, CSIC, CEA and POLIMI.

7.4 Conclusions

This deliverable shows the MSO thermal treatment process and its possibilities to decompose organic waste, especially IER. The technology is suited as a two-stage reactor system to fully decompose residual organics and completely oxidise flue gas into CO_2 and H_2O with only tracers of CO, SO_3 and NO_x. After releasing the waste molten salt into the water tank, the undissolved salt needs to be physically prepared for immobilisation. This process included air drying, grinding to fine particles, and drying in the drier. The waste was then analysed via XRD and XRF analysis. The moisture content was also determined. The XRD analysis showed that Natrite, Essenite, Trona and Thermonatrite mainly composite MSO waste.

The samples of this improved salt were sent to the PREDIS partners to study their immobilisation techniques.

REFERENCES

[30] Flandinet, L., Tedjar, F., Ghetta, V., & Fouletier, J. (2012). Metals recovering from waste printed circuit boards (WPCBs) using molten salts. Journal of Hazardous Materials, 213–214, 485–490. https://doi.org/10.1016/j.jhazmat.2012.02.037

[31] Lin, C., Chi, Y., Jin, Y., Jiang, X., Buekens, A., Zhang, Q., & Chen, J. (2018). Molten salt oxidation of organic hazardous waste with high salt content. https://doi.org/10.1177/0734242X17748364

[32] PANDETI, S., & BUCKLEY, S. G. (2004). MOLTEN SALT OXIDATION OF CHLOROBENZENE. Combustion Science and Technology, 176(2), 257–276. https://doi.org/10.1080/00102200490256171

[33] Yang, H.-C., Cho, Y.-Z., Eun, H.-C., & Kang, Y. (2008). Destruction of Trichloroethylene in a Two Stage Molten Salt Oxidation Reactor System. Journal of Chemical Engineering of Japan, 41(7), 597–601. https://doi.org/10.1252/jcej.07WE078

[34] Yang, H., Cho, Y., Eun, H., & Kim, E. (2019). Destruction of chlorinated organic solvents in a two-stage molten salt oxidation reactor system, (September 2007). https://doi.org/10.1016/j.ces.2007.01.055

[35] Yao, Z., Li, J., & Zhao, X. (2011). Molten salt oxidation: A versatile and promising technology for the destruction of organic-containing wastes. Chemosphere, 84(9), 1167–1174. https://doi.org/10.1016/j.chemosphere.2011.05.061

[36] Volkovich, V. A., Gri, T. R., Fields, M., & Fray, D. J. (1998). Oxidation of ceramic uranium dioxide in alkali metal carbonate-based melts : a study using various oxidants and comparison with UO2 powder. Journal of Nuclear Materials, 256(0022), 131–138.

[37] Yang, H., Cho, Y., Eun, H., & Kim, E. (2008). Destruction of chlorobenzene and carbon tetrachloride in a two-stage molten salt oxidation reactor system, 73. https://doi.org/10.1016/j.chemosphere.2008.03.045

[38] https://pubchem.ncbi.nlm.nih.gov/compound/Sodium-Carbonate#section=pH (cited 21.8.2023)